Lepton-nucleus scattering within Hartree-Fock (HF) and continuum Random Phase Approximation (CRPA) approach

Vishvas Pandey (University of Florida)

Natalie Jachowicz, Alexis Nikolakopoulos, Nils Van Dessel (Ghent University)

Neutrino Joint Theory-Experiment WG Meeting, Fermilab, March 9, 2020

AIM

- We use an unified microscopic many-body nuclear theory framework based on Hartree-Fock (HF) and continuum Random Phase Approximation (CRPA) approach to:

  - Calculate ground state properties of various nuclei (^{12}C, ^{16}O, ^{40}Ca, ^{40}Ar, ^{56}Fe and ^{208}Pb)
  - Calculate elastic electron-nucleus and coherent elastic neutrino-nucleus scattering (CEvNS) cross sections
  - Calculate electron- and (anti)neutrino-nucleus cross sections from low-energy excitations, giant resonances to quasielastic region
  - Study impact of these on various goals of neutrino experiments
  - Help and support neutrino experiments in achieving precision and new physics goals

Scope of this talk

Outline

- Calculating Lepton-Nucleus Cross Sections
- HF-CRPA Model
- Comparison with electron- and (anti)neutrino-nucleus data
- Understanding low-energy ν_e/ν_μ cross section differences

Scope of this talk

- Lepton-nucleus scattering

$\omega \lesssim$ **50 MeV**, $|\vec{\mathbf{q}}| \lesssim$ **300 MeV/c**

- Low-energy excitations and Giant Resonances
- Details of nuclear structure physics
- Supernova neutrinos

We describe this whole region in a self-consistent HF-CRPA approach

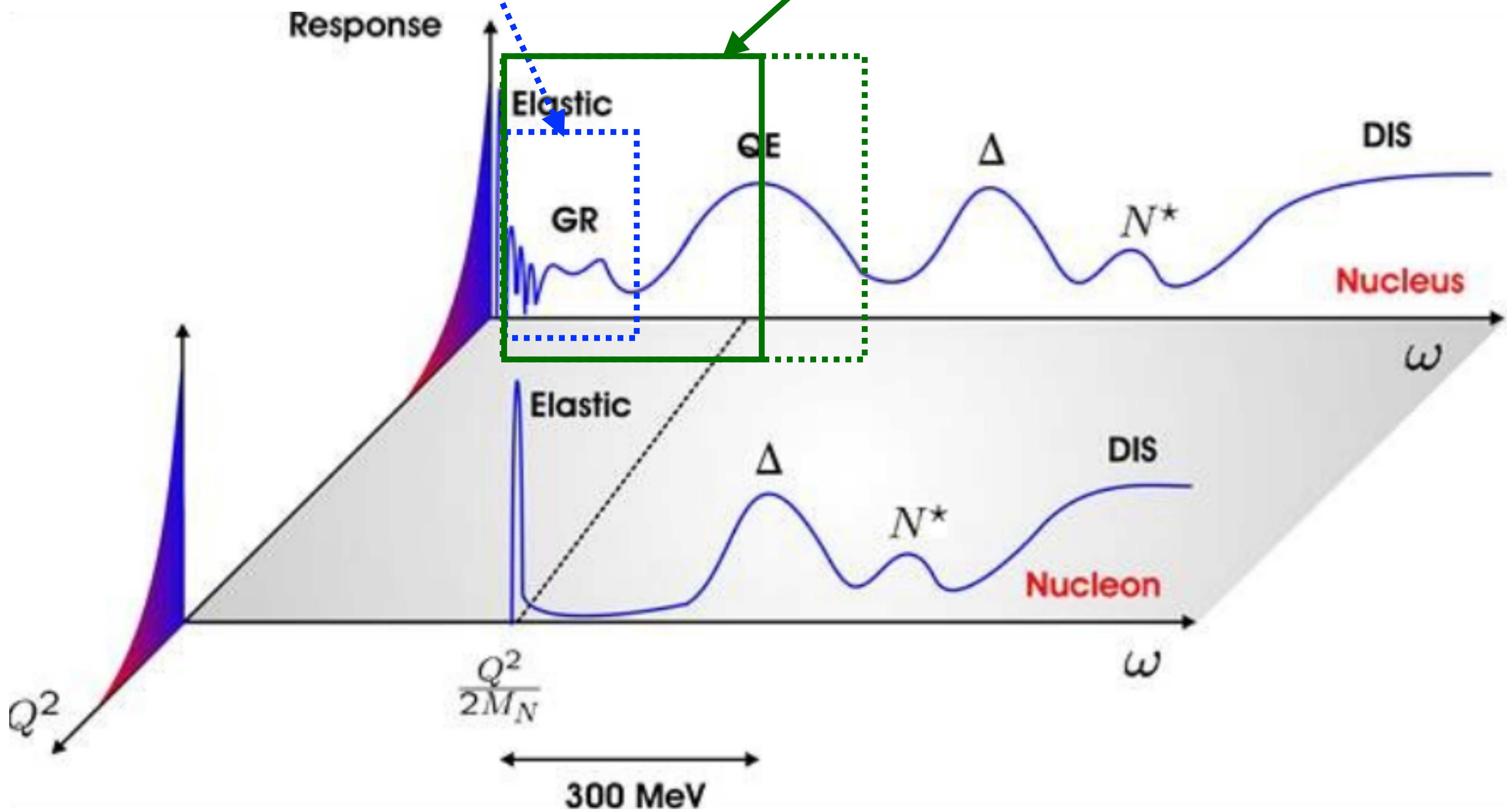

Outline

- Calculating Lepton-Nucleus Cross Sections
- HF-CRPA Model
- Comparison with electron- and (anti)neutrino-nucleus data
- Understanding low-energy ν_e/ν_μ cross section differences

Lepton-Nucleus Scattering

(e, e') scattering

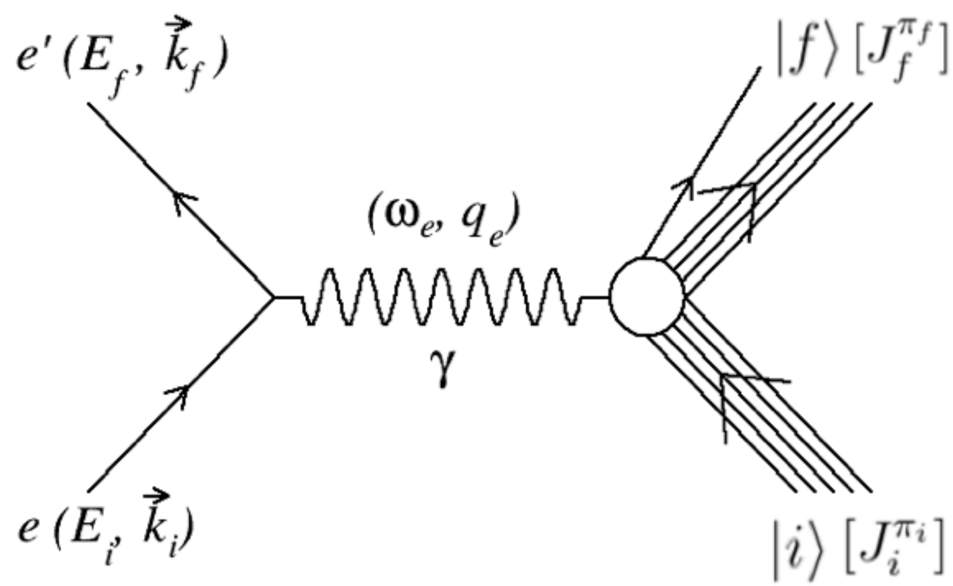

Kinematics: $\omega = E_i - E_f, \quad q = |\overrightarrow{k}_i - \overrightarrow{k}_f|, \quad Q^2 = q^2 - \omega^2$

Cross section: $d\sigma \approx |M_{fi}|^2 \approx |j_\mu \frac{1}{Q^2} J^\mu_{fi}|^2 \approx \frac{1}{Q^4} j^*_\mu j_\nu\ J^{\mu *}_{fi} J^{\nu *}_{fi}$

$$W^{\mu\nu} = \sum_f < i | J^{\mu\dagger} | f > < f | J^\nu | i > \ \ \delta(k_i - k_f)$$

$$\boxed{d\sigma \approx \frac{1}{Q^4} L_{\mu\nu} W^{\mu\nu}}$$

Lepton-Nucleus Scattering

(e, e') scattering

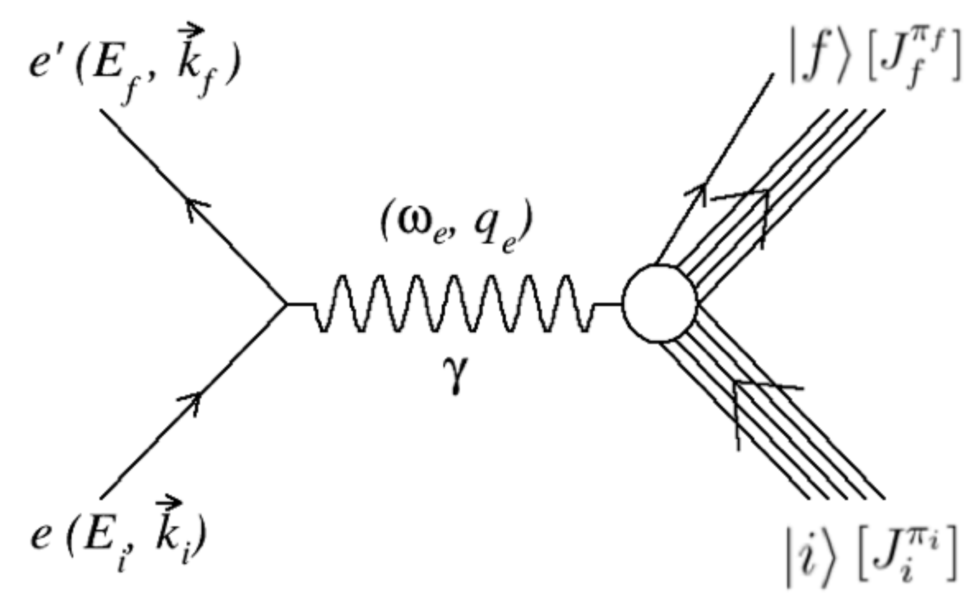

Kinematics: $\omega = E_i - E_f, \quad q = |\vec{k}_i - \vec{k}_f|, \quad Q^2 = q^2 - \omega^2$

Cross section: $d\sigma \approx |M_{fi}|^2 \approx |j_\mu \frac{1}{Q^2} J^\mu_{fi}|^2 \approx \frac{1}{Q^4} j^*_\mu j_\nu\, J^{\mu *}_{fi} J^{\nu *}_{fi}$

$$W^{\mu\nu} = \sum_f < i|J^{\mu\dagger}|f > < f|J^\nu|i > \;\; \delta(k_i - k_f)$$

$$\boxed{d\sigma \approx \frac{1}{Q^4} L_{\mu\nu} W^{\mu\nu}}$$

- Contracting the leptonic and hadronic tensor, we obtain a sum involving projections of the current matrix elements. It is convenient to choose these to be transverse and longitudinal with respect to the virtual photon direction. Thus we obtain structure of the form: $v_L\, R_L + v_T\, R_T$, where responses are functions of ω and q.

$$\boxed{\left(\frac{d^2\sigma}{d\omega_e d\Omega}\right)_e = \frac{\alpha^2}{Q^4}\left(\frac{2}{2J_i+1}\right)\frac{1}{k_f E_i}\;\zeta^2(Z', E_f, q_e)\left[\sum_{J=0}^{\infty}\sigma^J_{L,e} + \sum_{J=1}^{\infty}\sigma^J_{T,e}\right]}$$

$$\sigma_{L,e} = v_e^L R_e^L$$

$$\sigma_{T,e} = v_e^T R_e^T$$

- $\zeta^2(Z', E_f, q_e)$ takes care of the influence of the Coulomb field of nucleus on the outgoing charged lepton.
- σ_L and σ_T are summed over multipoles corresponds to discrete and continuum states of a nucleus having angular momentum and parity (J^π) as good quantum numbers.

Lepton-Nucleus Scattering

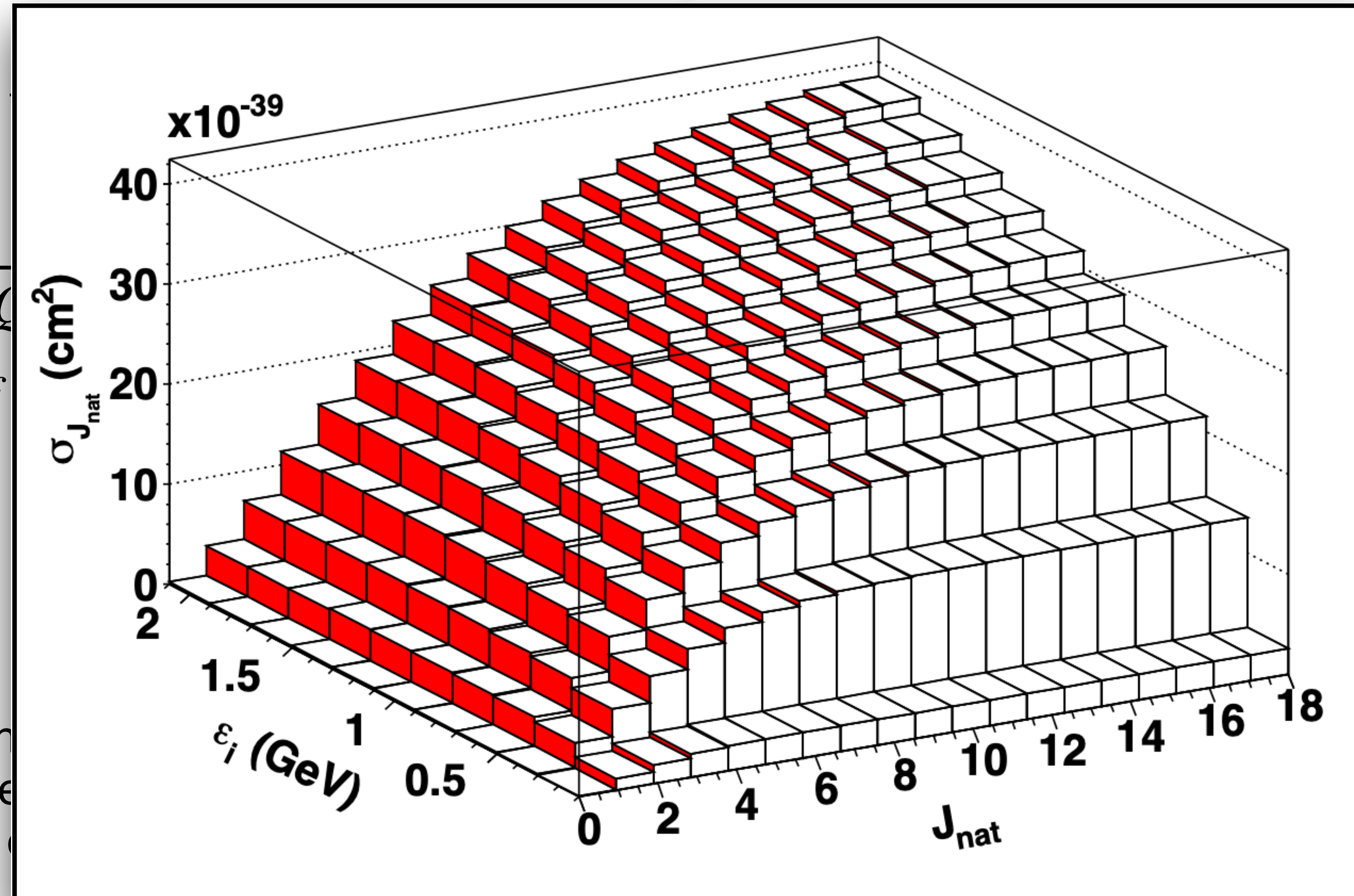

Kinematics: $\omega = E_i - E_f, \quad q = |$ ... $\rangle\, [J_f^{\pi_f}]$

Cross section: $d\sigma \approx |M_{fi}|^2 \approx |j_\mu$ ...

$$W^{\mu\nu} = \sum_f < i\,|\,J^{\mu\dagger}\,|\,f$$ ...

$[J_i^{\pi_i}]$

$$\boxed{d\sigma \approx \frac{1}{Q^4} L_{\mu\nu} W^{\mu\nu}}$$

- Contracting the leptonic and hadron ... elements. It is convenient to choose ... hoton direction. Thus we obtain structure ... .

$$\boxed{\left(\frac{d^2\sigma}{d\omega_e d\Omega}\right)_e = \frac{\alpha^2}{Q^4}\left(\frac{2}{2J_i+1}\right)\frac{1}{k_f E_i}\;\zeta^2(Z', E_f, q_e)\left[\sum_{J=0}^{\infty}\sigma^J_{L,e} + \sum_{J=1}^{\infty}\sigma^J_{T,e}\right]}$$

$$\sigma_{L,e} = v_e^L R_e^L$$

$$\sigma_{T,e} = v_e^T R_e^T$$

- ζ^2 *(Z', E_f, q_e)* takes care of the influence of the Coulomb field of nucleus on the outgoing charged lepton.
- σ_L and σ_T are summed over multipoles corresponds to discrete and continuum states of a nucleus having angular momentum and parity *(J^π)* as good quantum numbers.

VP, N. Jachowicz, T. Van Cuyck, J. Ryckebusch, M. Martini, Phys. Rev. C92, 024606 (2015)

Lepton-Nucleus Scattering

(e, e') scattering

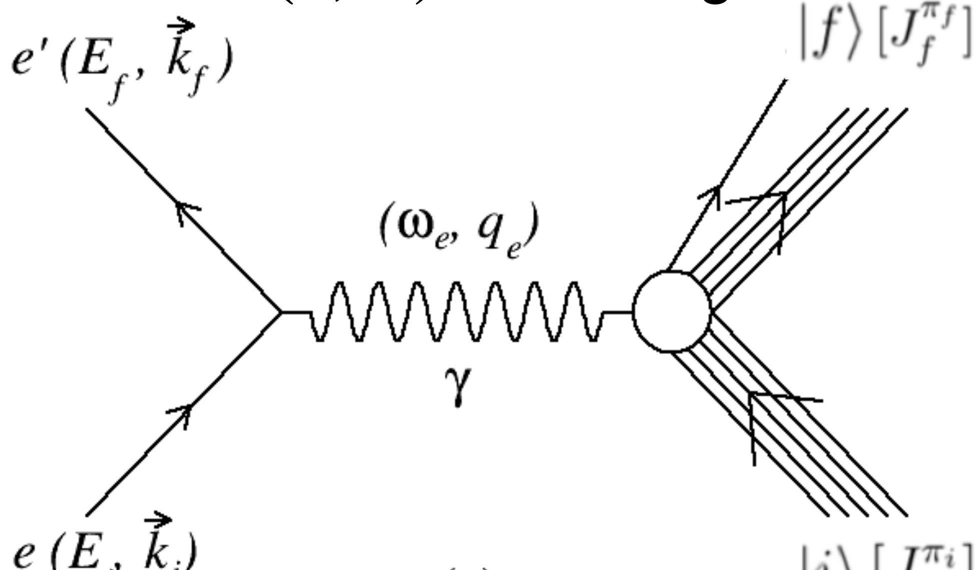

(a)

$$\boxed{\begin{aligned}\left(\frac{d^2\sigma}{d\omega_e d\Omega}\right)_e &= \frac{\alpha^2}{Q^4}\left(\frac{2}{2J_i+1}\right)\frac{1}{k_f E_i} \\ &\times\ \zeta^2\left(Z', E_f, q_e\right)\left[\sum_{J=0}^{\infty}\sigma_{L,e}^J + \sum_{J=1}^{\infty}\sigma_{T,e}^J\right]\end{aligned}}$$

$$\sigma_{L,e} = v_e^L R_e^L$$

$$\sigma_{T,e} = v_e^T R_e^T$$

v's → Leptonic coefficients → Purely kinematical

R's → Response functions → Nuclear dynamics → **Need nuclear models to calculate!**

Lepton-Nucleus Scattering

- **The vector current is conserved between electromagnetic and weak response (CVC).**

(e, e') scattering

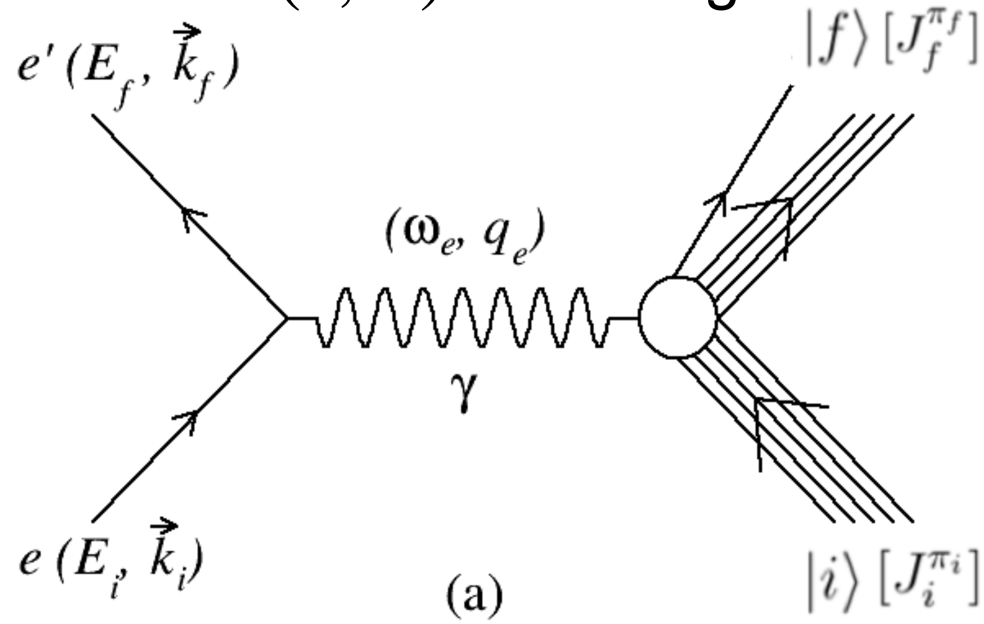

(a)

(ν_l, l^-) scattering

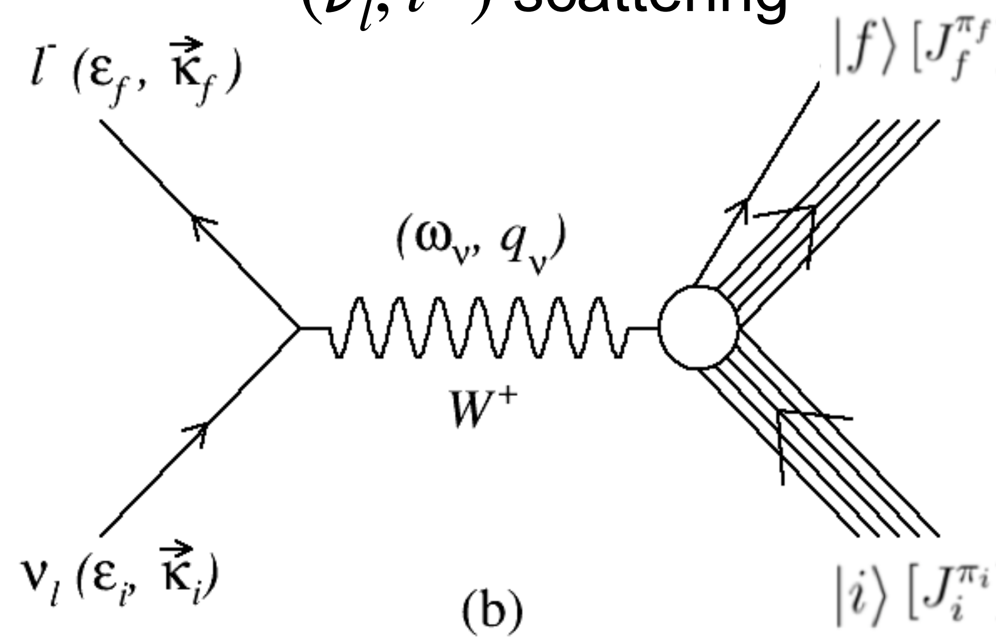

(b)

$$\boxed{\begin{aligned}\left(\frac{d^2\sigma}{d\omega_e d\Omega}\right)_e &= \frac{\alpha^2}{Q^4} \left(\frac{2}{2J_i+1}\right) \frac{1}{k_f E_i} \\ &\times \zeta^2(Z', E_f, q_e) \left[\sum_{J=0}^{\infty} \sigma_{L,e}^J + \sum_{J=1}^{\infty} \sigma_{T,e}^J\right]\end{aligned}}$$

$$\boxed{\begin{aligned}\left(\frac{d^2\sigma}{d\omega_\nu d\Omega}\right)_\nu &= \frac{G_F^2 \cos^2\theta_c}{(4\pi)^2} \left(\frac{2}{2J_i+1}\right) \varepsilon_f \kappa_f \\ &\times \zeta^2(Z', \varepsilon_f, q_\nu) \left[\sum_{J=0}^{\infty} \sigma_{CL,\nu}^J + \sum_{J=1}^{\infty} \sigma_{T,\nu}^J\right]\end{aligned}}$$

$$\sigma_{L,e} = v_e^L R_e^L$$
$$\sigma_{T,e} = v_e^T R_e^T$$

$$\sigma_{CL,\nu}^J = \left[v_\nu^{\mathcal{M}} R_\nu^{\mathcal{M}} + v_\nu^{\mathcal{L}} R_\nu^{\mathcal{L}} + 2\, v_\nu^{\mathcal{ML}} R_\nu^{\mathcal{ML}}\right]$$
$$\sigma_{T,\nu}^J = \left[v_\nu^T R_\nu^T \underset{\downarrow}{\pm} 2\, v_\nu^{TT} R_\nu^{TT}\right]$$

sign is the only difference between ν and anti-ν

v's → Leptonic coefficients → Purely kinematical

R's → Response functions → Nuclear dynamics → **Need nuclear models to calculate!**

Outline

- Calculating Lepton-Nucleus Cross Sections
- HF-CRPA Model
- Comparison with electron- and (anti)neutrino-nucleus data
- Understanding low-energy ν_e/ν_μ cross section differences

HF-CRPA Approach [Ghent Model]

- **Base-model: Hartree-Fock**
  - We use Hartree-Fock (HF) method with a Skyrme (SkE2) potential and solve the Schrodinger equation to obtain single-particle wave functions filling all the single-particle states up to the Fermi level for all the nucleons in the nucleus.
    - HF ground state: All single-particle states filled up to the Fermi-level and all higher-lying states being empty.
    - HF excited state: Where a single nucleon, a “particle”, occupied the level above the fermi surface, leaving behind a “hole” in the Fermi sea, i.e. 1p-1h state.

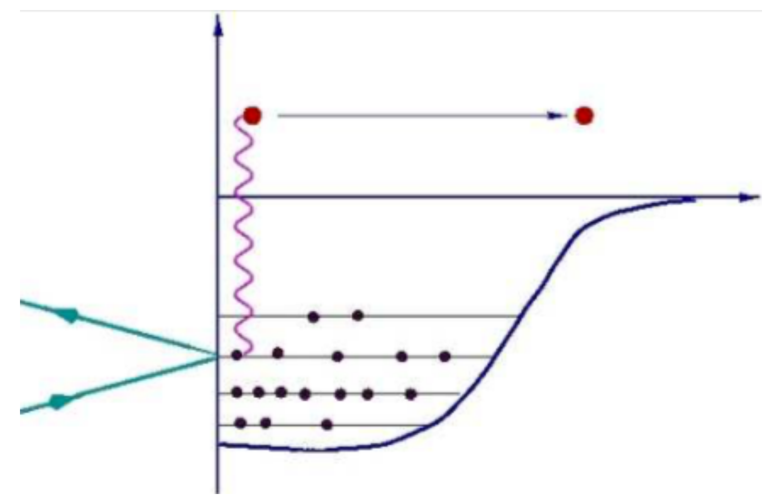

HF-CRPA Approach [Ghent Model]

- **Base-model: Hartree-Fock**

  - We use Hartree-Fock (HF) method with a Skyrme (SkE2) potential and solve the Schrodinger equation to obtain single-particle wave functions filling all the single-particle states up to the Fermi level for all the nucleons in the nucleus.

    - HF ground state: All single-particle states filled up to the Fermi-level and all higher-lying states being empty.

    - HF excited state: Where a single nucleon, a "particle", occupied the level above the fermi surface, leaving behind a "hole" in the Fermi sea, i.e. 1p-1h state.

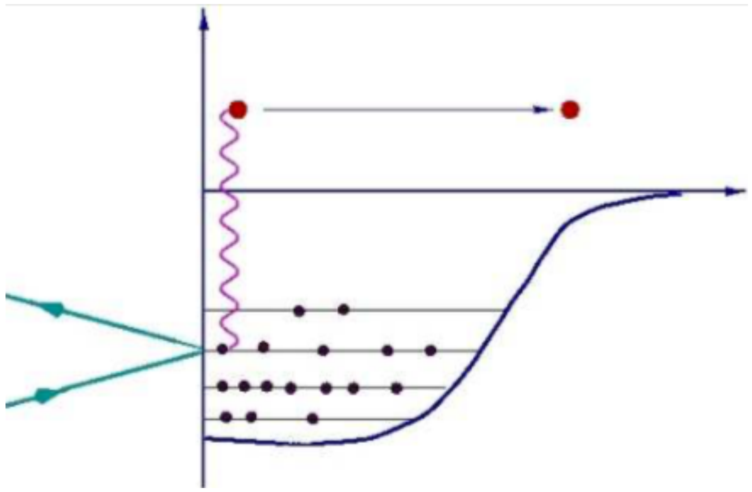

- When probing the excitation region lying at 10s of MeV in nuclei, some states are found to have much larger strength than predicted on the basis of a transition from the ground state to a 1p-1h state. This is the region of so-called giant resonances (GR).

- The large strength and location of these excitations point to the fact that GR are collective excitations involving the cooperative participation of several nucleons in contrast to 1p-1h excitations and thus require a more sophisticated treatment => inclusion of long-range correlations between nucleons and a RPA treatment.

HF-CRPA Approach [Ghent Model]

- **Continuum random phase approximation**

  - The CRPA approach describes a nuclear excited state as the linear combination of particle-hole (*ph*⁻¹) and hole-particle (*hp*⁻¹) excitations out of a correlated nuclear ground state:

$$|\Psi^C_{RPA}\rangle = \sum_{C'} \left\{ X_{C,C'} \; |p'h'^{-1}\rangle - Y_{C,C'} \; |h'p'^{-1}\rangle \right\}$$

  - We solve CRPA equations using a Green's function approach which allows one to treat the single-particle energy continuum exactly by solving the RPA equations in coordinate space.

HF-CRPA Approach [Ghent Model]

- **Continuum random phase approximation**

  - The CRPA approach describes a nuclear excited state as the linear combination of particle-hole (ph^{-1}) and hole-particle (hp^{-1}) excitations out of a correlated nuclear ground state:

$$|\Psi^C_{RPA}\rangle = \sum_{C'} \left\{ X_{C,C'} \; |p'h'^{-1}\rangle - \; Y_{C,C'} \; |h'p'^{-1}\rangle \right\}$$

  - We solve CRPA equations using a Green's function approach which allows one to treat the single-particle energy continuum exactly by solving the RPA equations in coordinate space.

  - The propagation of particle-hole pairs in the nuclear medium is described by the polarization propagator. In the Lehmann representation, this particle-hole Green's function is given by

$$\Pi(x_1, x_2, x_3, x_4; E_x) \;\; = \;\; \hbar \sum_n \left[\frac{\langle\Psi_0|\hat{\psi}^\dagger(x_2)\hat{\psi}(x_1)|\Psi_n\rangle\langle\Psi_n|\hat{\psi}^\dagger(x_3)\hat{\psi}(x_4)|\Psi_0\rangle}{E_x - (E_n - E_o) + i\eta} - \frac{\langle\Psi_0|\hat{\psi}^\dagger(x_3)\hat{\psi}(x_4)|\Psi_n\rangle\langle\Psi_n|\hat{\psi}^\dagger(x_2)\hat{\psi}(x_1)|\Psi_0\rangle}{E_x + (E_n - E_o) - i\eta} \right]$$

The first term represents particle states above Fermi level, second term represents hole states below Fermi level.

HF-CRPA Approach [Ghent Model]

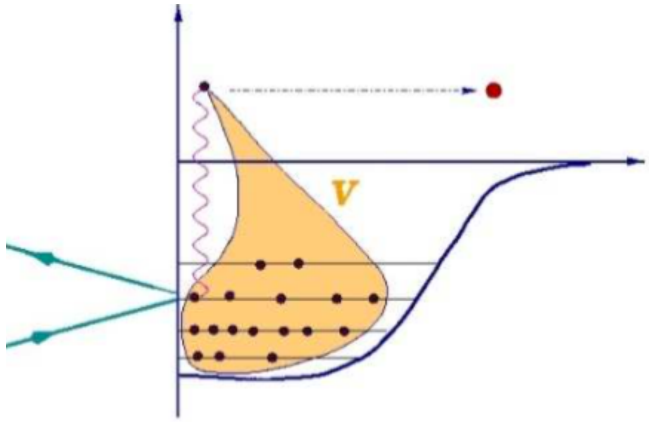

Continuum random phase approximation

- The local RPA-polarization propagator is obtained by an iteration to all orders of the first order contribution to the particle-hole Green's function.

$$\Pi^{(RPA)}(x_1, x_2; E_x) = \Pi^{(0)}(x_1, x_2; E_x) + \frac{1}{\hbar}\int dx dx' \, \Pi^0(x_1, x; E_x) \times \tilde{V}(x, x') \, \Pi^{(RPA)}(x', x_2; E_x)$$

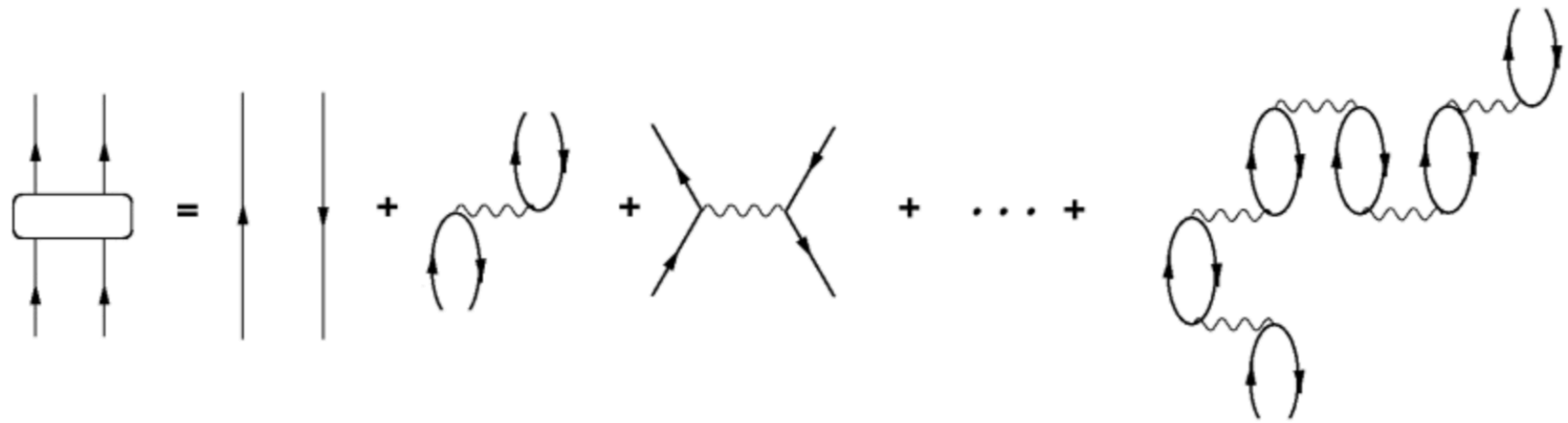

- The Skyrme (SkE2) nucleon-nucleon interaction, which was used in the HF calculations, is also used to perform CRPA calculations making this approach self-consistent.

- CRPA results are generally seen to reflect the q dependence of the data for momentum transfers ranging up to about ≲ 400 MeV/c (or, ω ≲ 50 MeV) and show the general characteristics of the excitation spectrum.

- HF-CRPA approach naturally includes: Binding, Fermi motion, elastic Final State Interaction (distortion of the outgoing nucleon in real MF potential), Pauli blocking, and orthogonality (both bound and scattered nucleon wave-functions are computed in the same nuclear potential).

Outline

- Calculating Lepton-Nucleus Cross Sections
- HF-CRPA Model
- Comparison with electron- and (anti)neutrino-nucleus data
- Understanding low-energy ν_e/ν_μ cross section differences

Comparison with (e,e') data on ^{12}C, ^{16}O, and ^{40}Ca

Comparison with (e,e') data on ^{12}C, ^{16}O, and ^{40}Ca

- **$^{12}C(e,e')$ cross sections**
  - Range of three momentum transfer at the QE peak: $100\ MeV \lesssim |q| \lesssim 1000\ MeV$

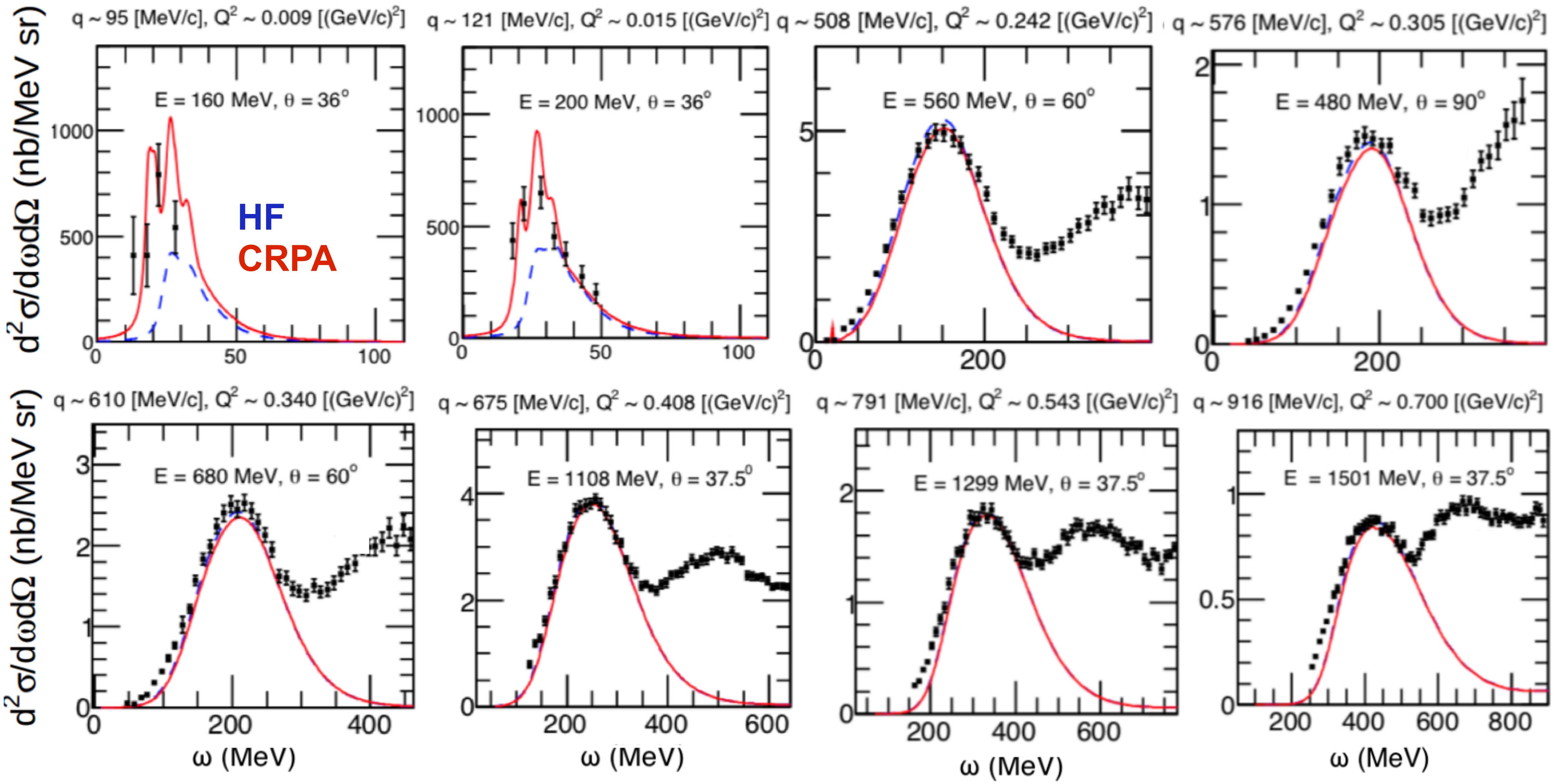

VP, N. Jachowicz, T. Van Cuyck, J. Ryckebusch, M. Martini, Phys. Rev. C92, 024606 (2015)

Data from:

D. Zeller, DESY-F23-73-2 (1973); P. Barreau et al., Nucl. Phys. A402, 515 (1983); J. S. O'Connell et al., Phys. Rev. C35, 1063 (1987); D. S. Bagdasaryan et al., YERPHI-1077-40-88 (1988); R. M. Sealock et al., Phys. Rev. Lett.62, 1350 (1989); D. B. Day et al., Phys. Rev. C 48, 1849 (1993); M. Anghinolfi et al., Nucl. Phys. A602, 405 (1996); J. Jourdan, Nucl. Phys. A603, 117 (1996); C. F. Williamsonet al., Phys. Rev. C56, 3152 (1997)

Comparison with (e,e') data on ^{12}C, ^{16}O, and ^{40}Ca

- **$^{12}C(e,e')$ R_L and R_T**

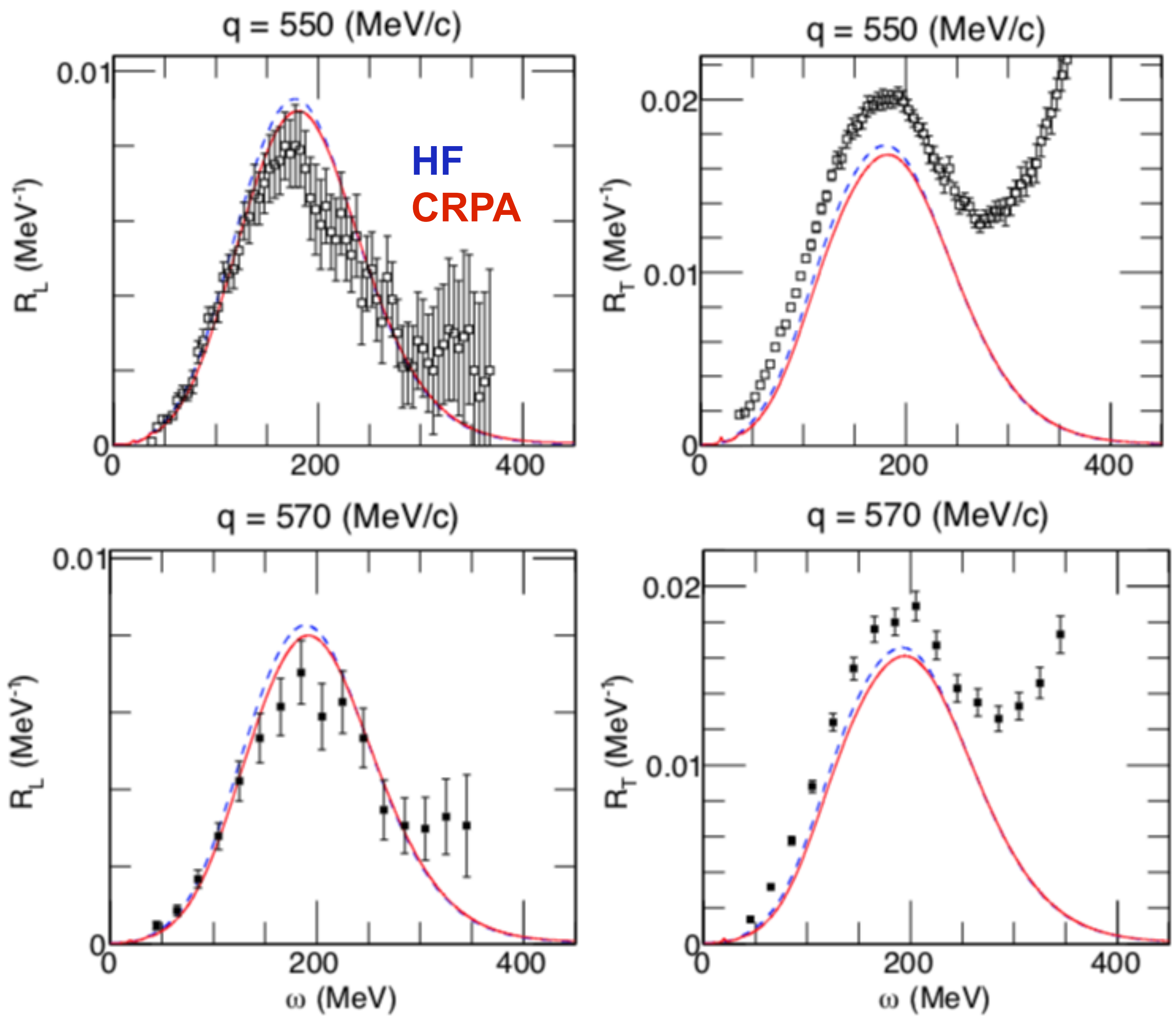

VP, N. Jachowicz, T. Van Cuyck, J. Ryckebusch, M. Martini, Phys. Rev. C92, 024606 (2015)

Data from:

D. Zeller, DESY-F23-73-2 (1973); P. Barreau et al., Nucl. Phys. A402, 515 (1983); J. S. O'Connell et al., Phys. Rev. C35, 1063 (1987); D. S. Bagdasaryan et al., YERPHI-1077-40-88 (1988); R. M. Sealock et al., Phys. Rev. Lett.62, 1350 (1989); D. B. Day et al., Phys. Rev. C 48, 1849 (1993); M. Anghinolfi et al., Nucl. Phys. A602, 405 (1996); J. Jourdan, Nucl. Phys. A603, 117 (1996); C. F. Williamsonet al., Phys. Rev. C56, 3152 (1997)

Comparison with (e,e') data on ^{12}C, ^{16}O, and ^{40}Ca

- **^{16}O(e,e') and ^{40}Ca(e,e') cross sections**

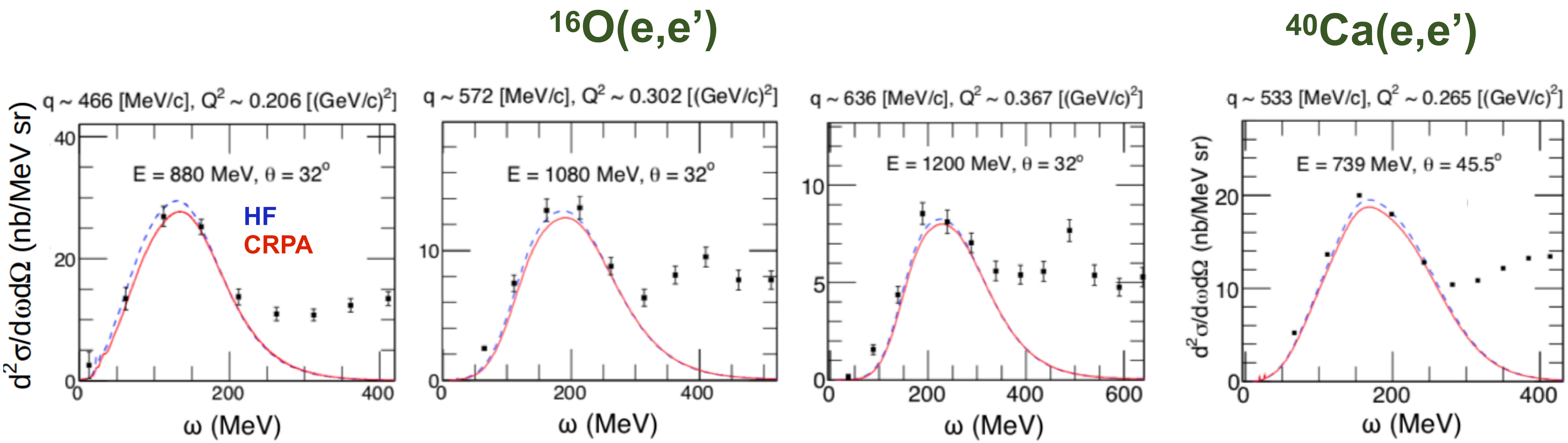

VP, N. Jachowicz, T. Van Cuyck, J. Ryckebusch, M. Martini, Phys. Rev. C92, 024606 (2015)

Data from:

D. Zeller, DESY-F23-73-2 (1973); P. Barreau et al., Nucl. Phys. A402, 515 (1983); J. S. O'Connell et al., Phys. Rev. C35, 1063 (1987); D. S. Bagdasaryan et al., YERPHI-1077-40-88 (1988); R. M. Sealock et al., Phys. Rev. Lett.62, 1350 (1989); D. B. Day et al., Phys. Rev. C 48, 1849 (1993); M. Anghinolfi et al., Nucl. Phys. A602, 405 (1996); J. Jourdan, Nucl. Phys. A603, 117 (1996); C. F. Williamsonet al., Phys. Rev. C56, 3152 (1997)

Comparison with (anti)neutrino data

$^{12}C(\nu_\mu, \mu^-)$ cross section (per neutron)

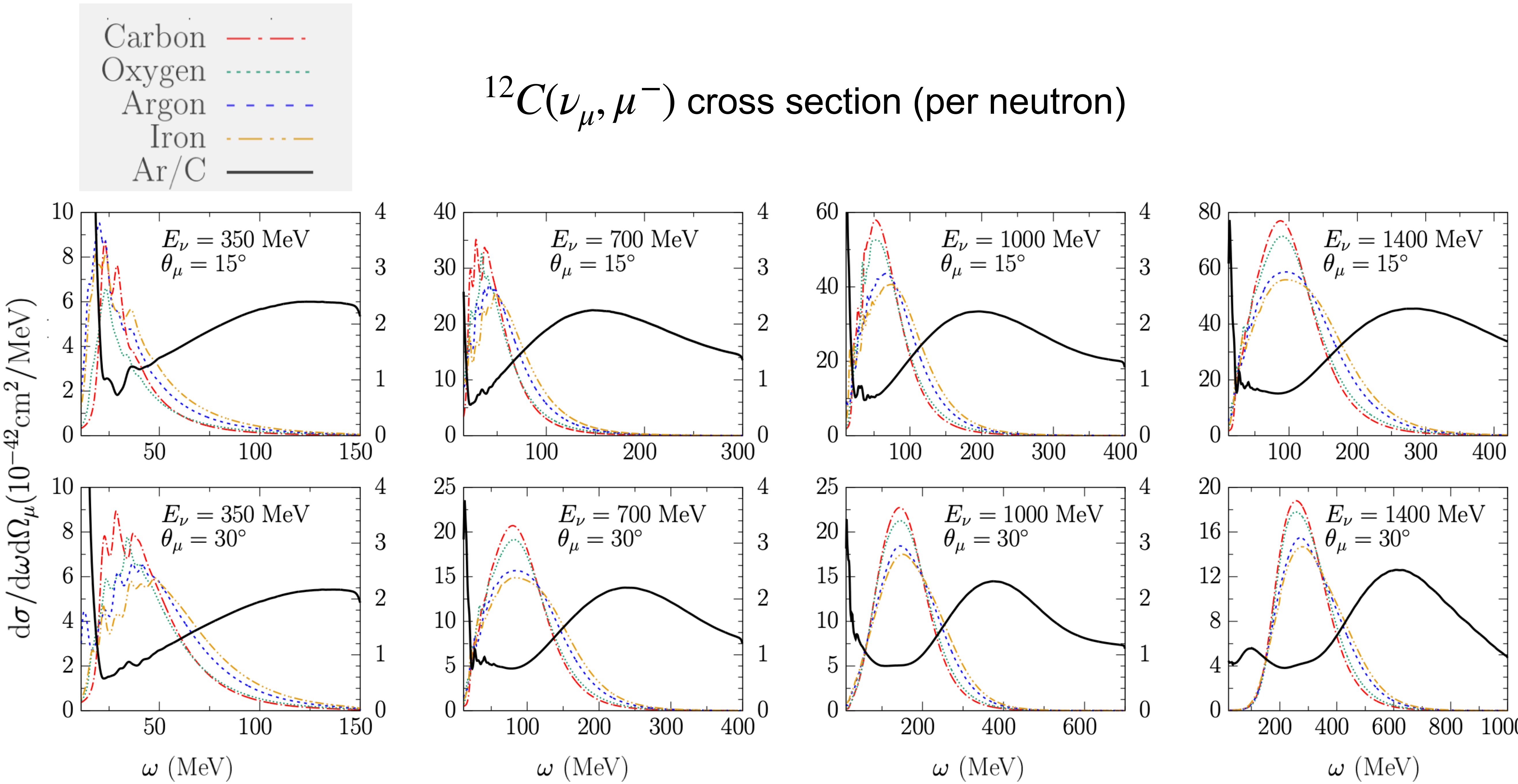

N. Van Dessel, N. Jachowicz, R. González-Jiménez, VP, T. Van Cuyck, Phys. Rev. C97, 044616 (2018)

Comparison with (anti)neutrino data

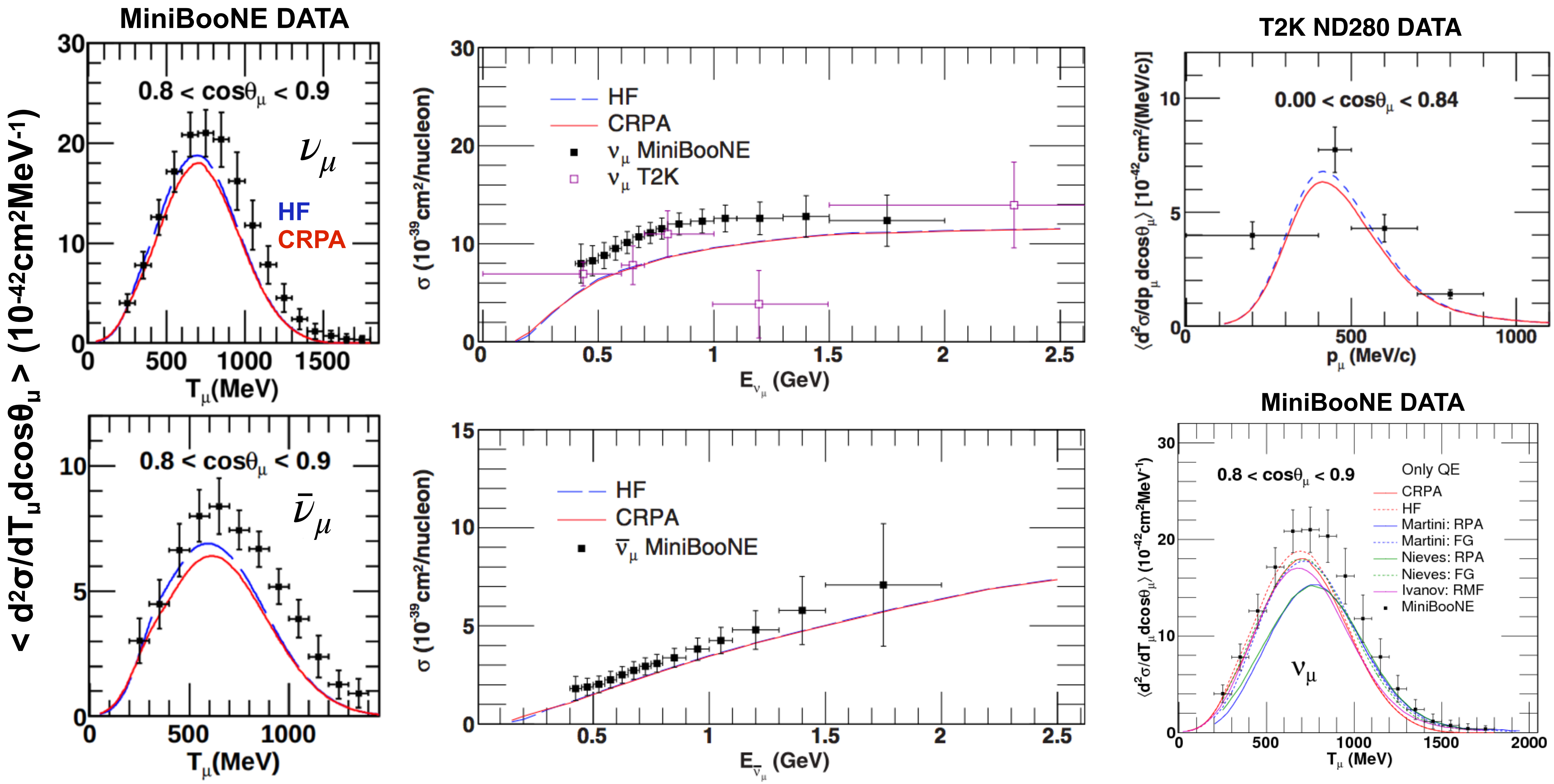

VP, N. Jachowicz, M. Martini, R. González Jiménez, J. Ryckebusch, T. Van Cuyck, and N. Van Dessel, Phys. Rev. C94, 054609 (2016)

Outline

- Calculating Lepton-Nucleus Cross Sections
- HF-CRPA Model
- Comparison with electron- and (anti)neutrino-nucleus data
- Understanding low-energy ν_e/ν_μ cross section differences

Low-Energy Lepton-Nucleus Scattering

- **Electron-nucleus scattering**

- Need sophisticated nuclear structure physics

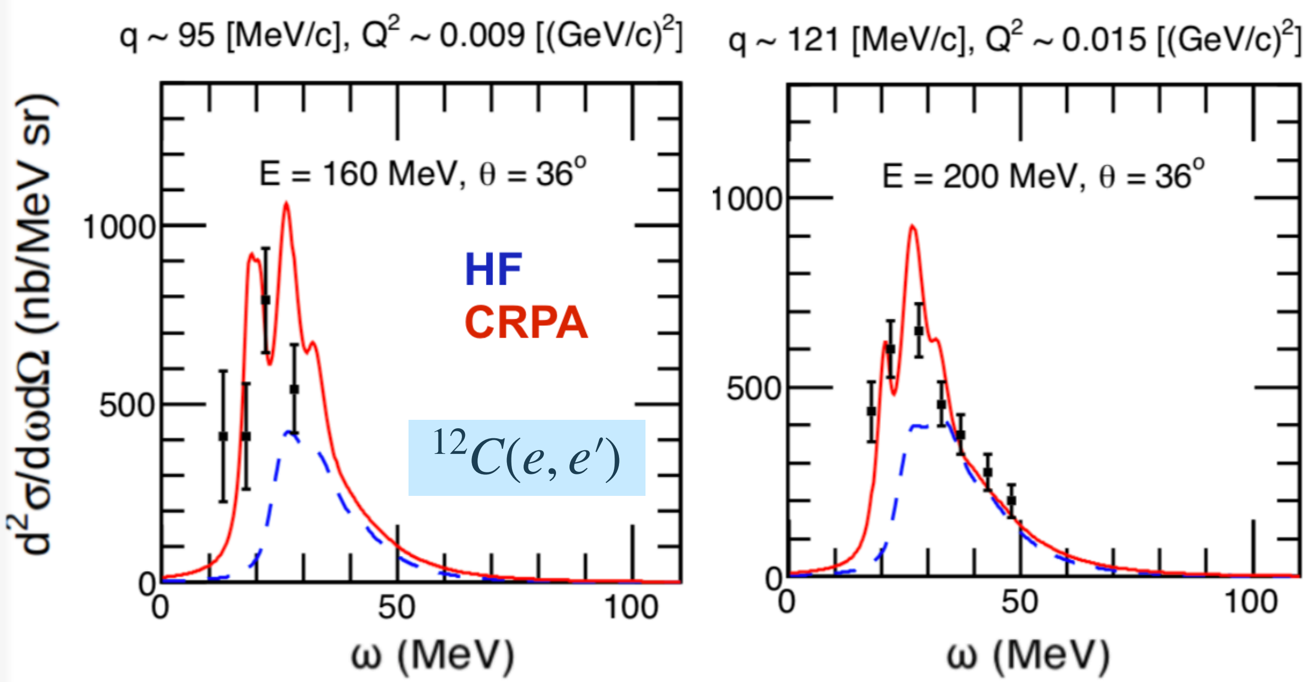

VP, N. Jachowicz, T. Van Cuyck, J. Ryckebusch, M. Martini, Phys. Rev. C92, 024606 (2015)

- **Electron-nucleus scattering**

- Need sophisticated nuclear structure physics

- Not Fermi-gas type models (that are in generators)

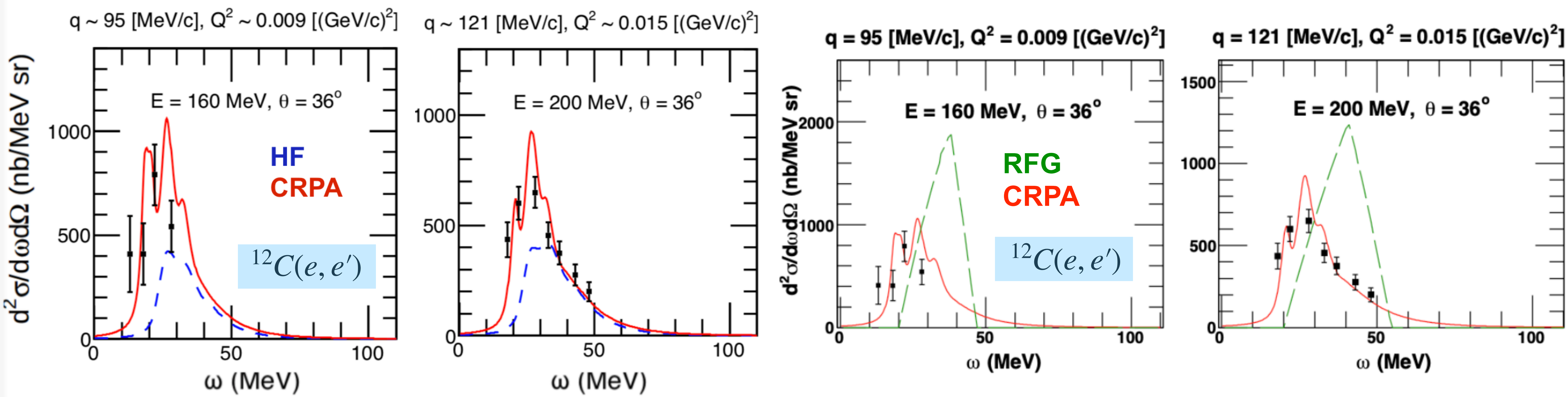

VP, N. Jachowicz, T. Van Cuyck, J. Ryckebusch, M. Martini, Phys. Rev. C92, 024606 (2015)

Low-Energy Lepton-Nucleus Scattering

• Electron-nucleus scattering

- Need sophisticated nuclear structure physics

- Not Fermi-gas type models (that are in generators)

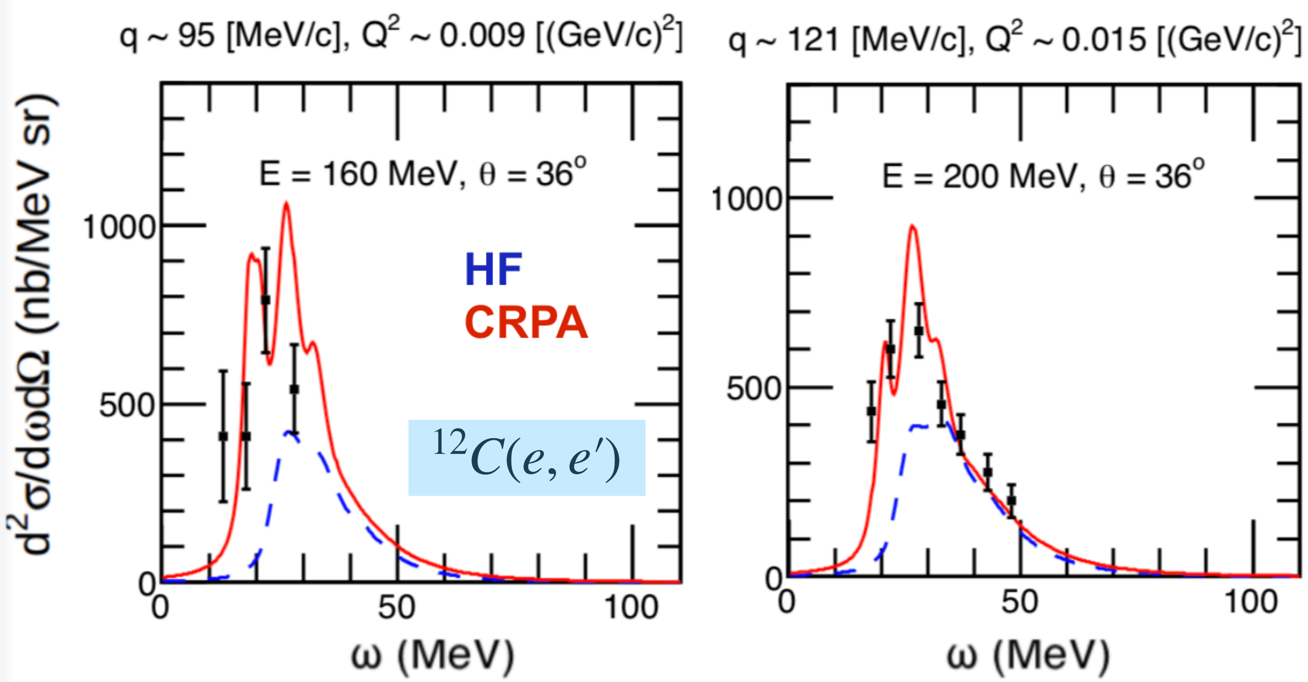

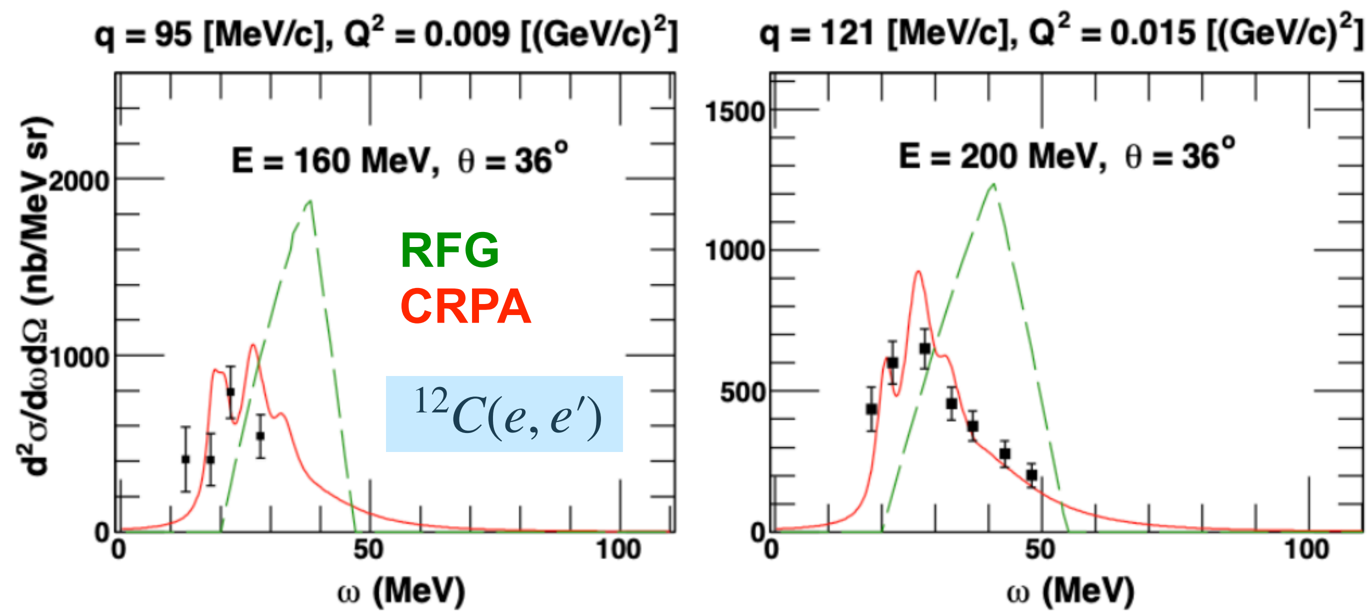

VP, N. Jachowicz, T. Van Cuyck, J. Ryckebusch, M. Martini, Phys. Rev. C92, 024606 (2015)

• Neutrino-nucleus scattering, comparison with GENIE

$\nu_e, \nu_\mu -$ ^{12}C *cross section*

- Working with Steven Gardiner …

$E = 200\ MeV,\ \theta = 8^o$

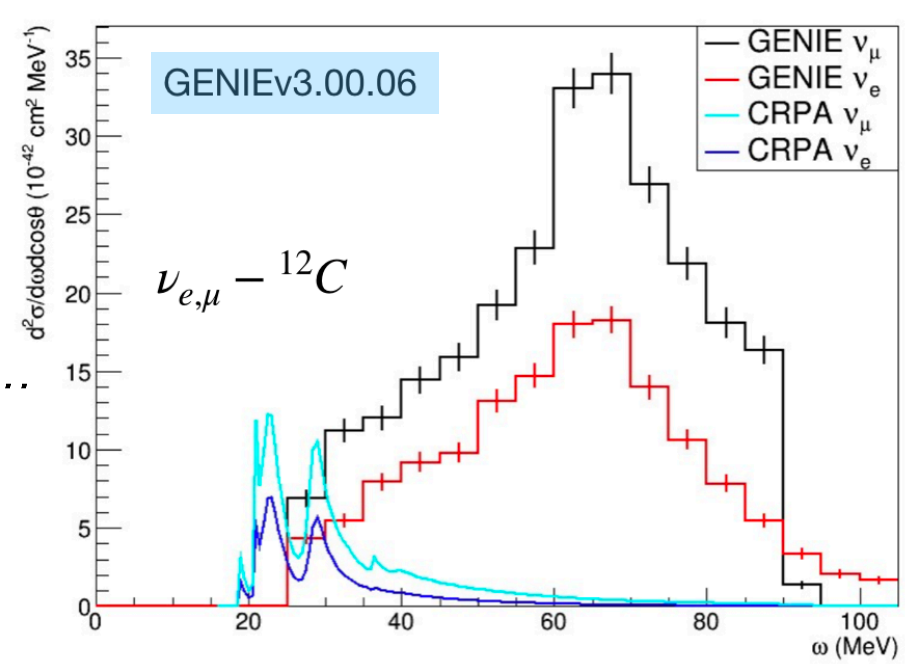

$E = 200\ MeV,\ \theta = 55^o$

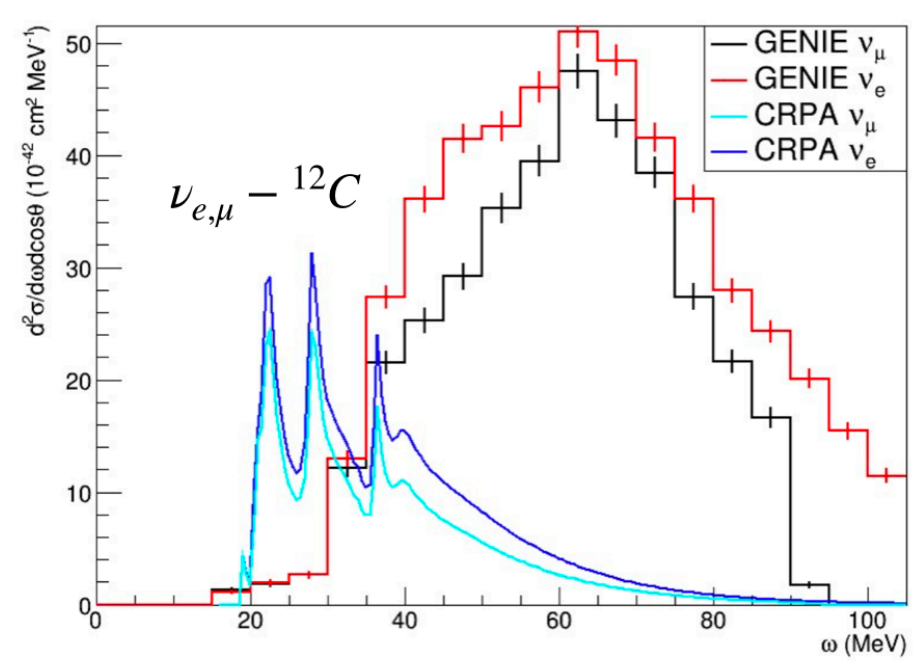

$^{12}C(\nu_\mu, \mu^-)$ scattering

- In neutrino experiments, we don't know ω, so let's look at things through outgoing lepton kinematics. For a given neutrino energy E_ν, cross sections as a function of muon energy T_μ, and scattering angle θ_μ.

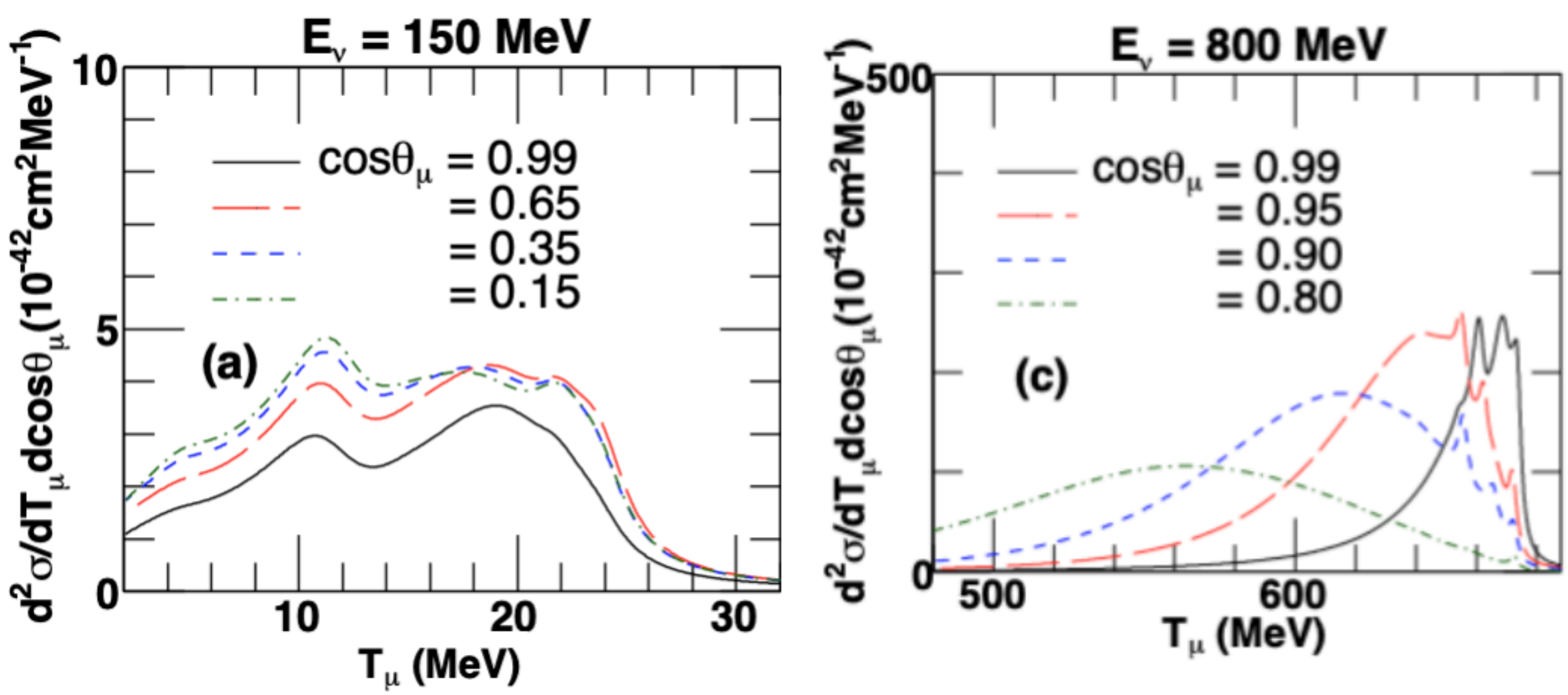

VP, N. Jachowicz, T. Van Cuyck, J. Ryckebusch, M. Martini, Phys. Rev. C92, 024606 (2015)

- Low E_ν: cross section is dominated by low-energy excitations.
- E_ν = 800 MeV: forward scattering receive contribution from low-energy excitations.

Flux-folded cross section

- Cross sections (on ^{12}C) for a fixed $\cos\theta_\mu = 0.97$ and for fixed neutrino energies from 300 MeV to 1000 MeV, weighted with the T2K ν_μ flux and plotted as a function of p_μ.

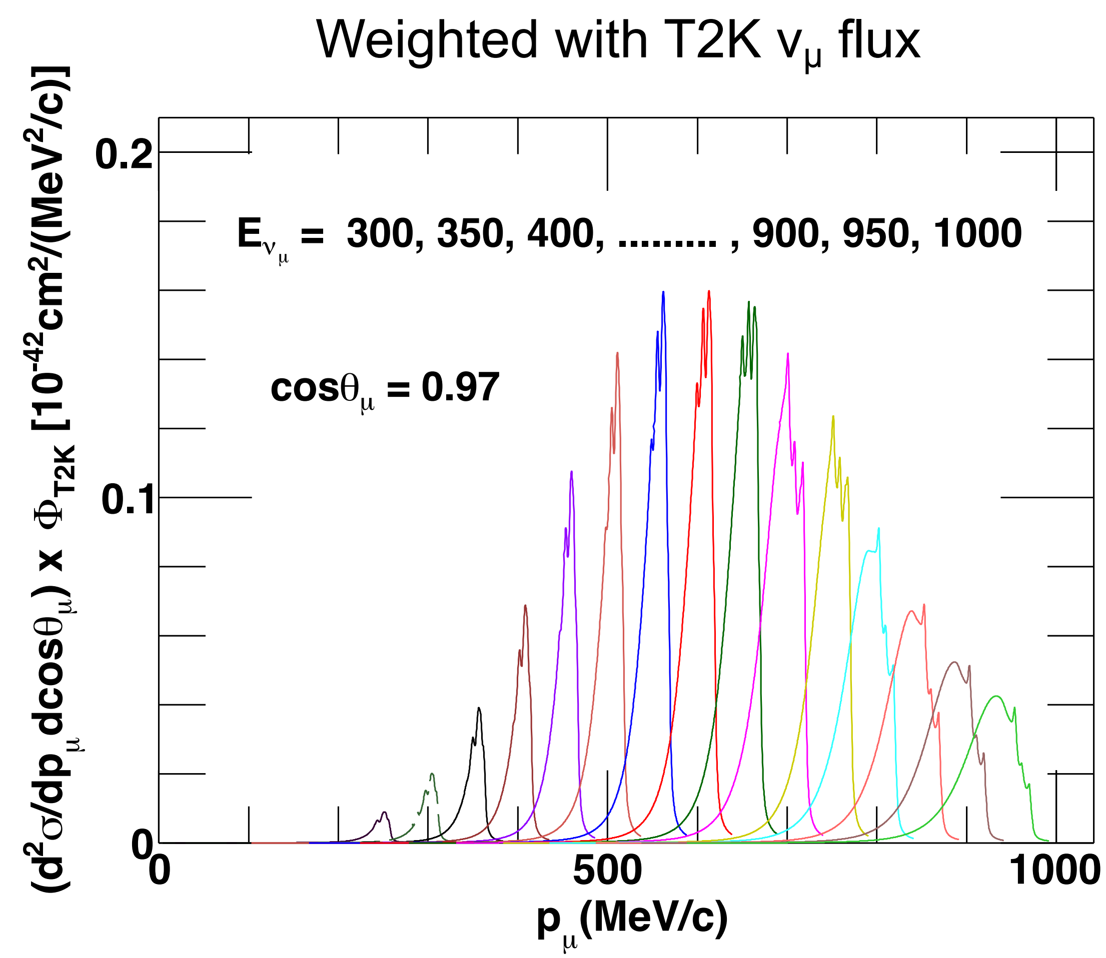

VP, N. Jachowicz, M. Martini, R. González-Jiménez, J. Ryckebusch, T. Van Cuyck, N. Van Dessel, Phys. Rev. C94, 054609 (2016).

Flux-folded cross section

- Cross sections (on ^{12}C) for a fixed $\cos\theta_\mu = 0.97$ and for fixed neutrino energies from 300 MeV to 1000 MeV, weighted with the T2K ν_μ flux and plotted as a function of p_μ.
- Integrating over energies (BNB flux-folded), the peaks disappear but the significant contributions of low-energy excitations (ω < 50 MeV) stays at forward scattering.

Weighted with T2K ν_μ flux

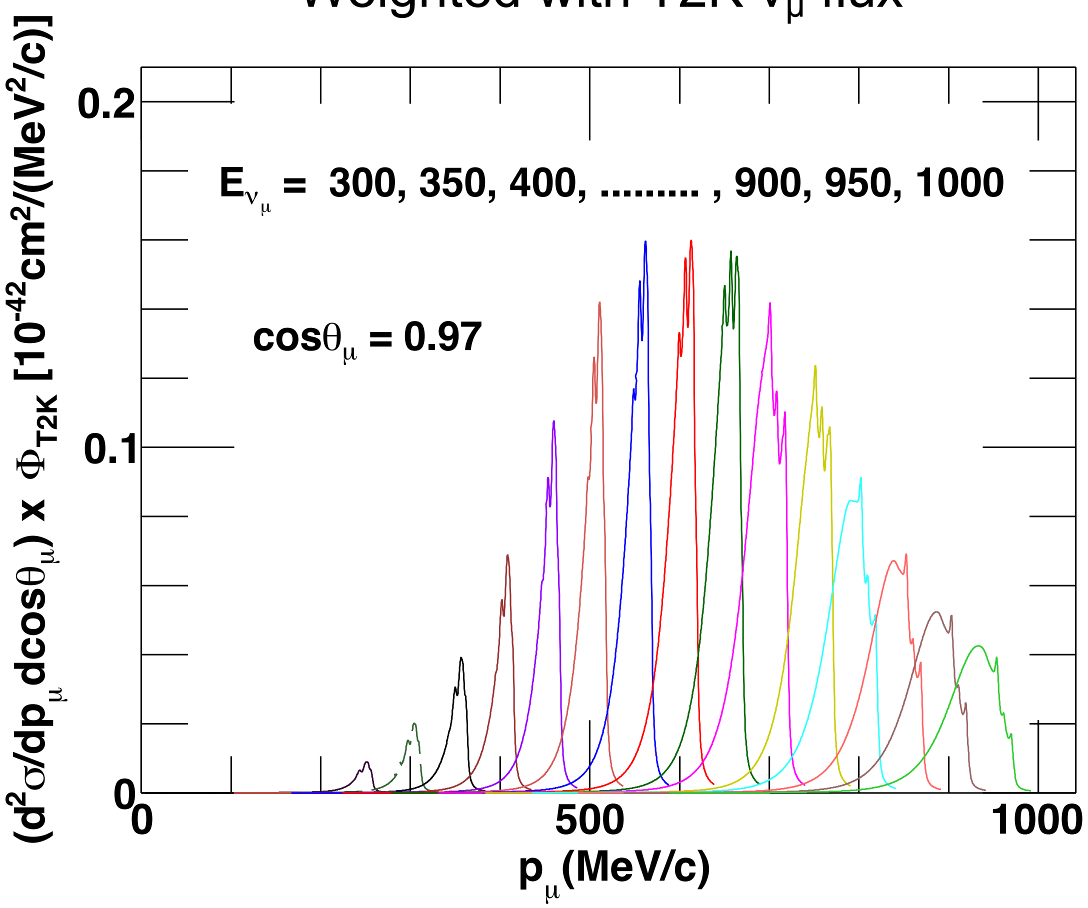

VP, N. Jachowicz, M. Martini, R. González-Jiménez, J. Ryckebusch, T. Van Cuyck, N. Van Dessel, Phys. Rev. C94, 054609 (2016).

Folded with BNB ν_μ flux

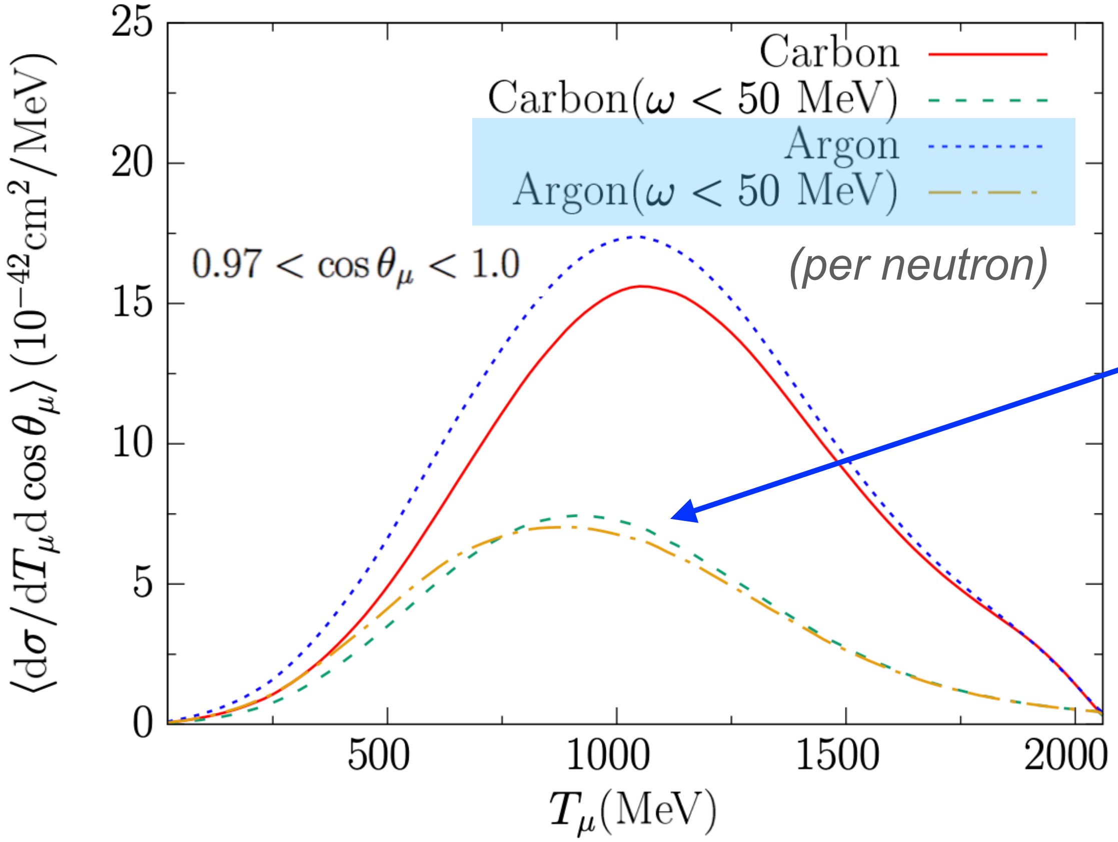

- Significant contribution from low-energy excitations (ω < 50 MeV)

N. Van Dessel, N. Jachowicz, R. González-Jiménez, VP, T. Van Cuyck, Phys. Rev. C97, 044616 (2018).

ν_e/ν_μ cross sections at low energies

- At lower energies:
  - For small scattering angles, ν_μ cross sections are higher than the ν_e ones.
  - For larger scattering angles, this behavior is opposite.

- At higher energies:
  - ν_e and ν_μ cross sections roughly coincide.

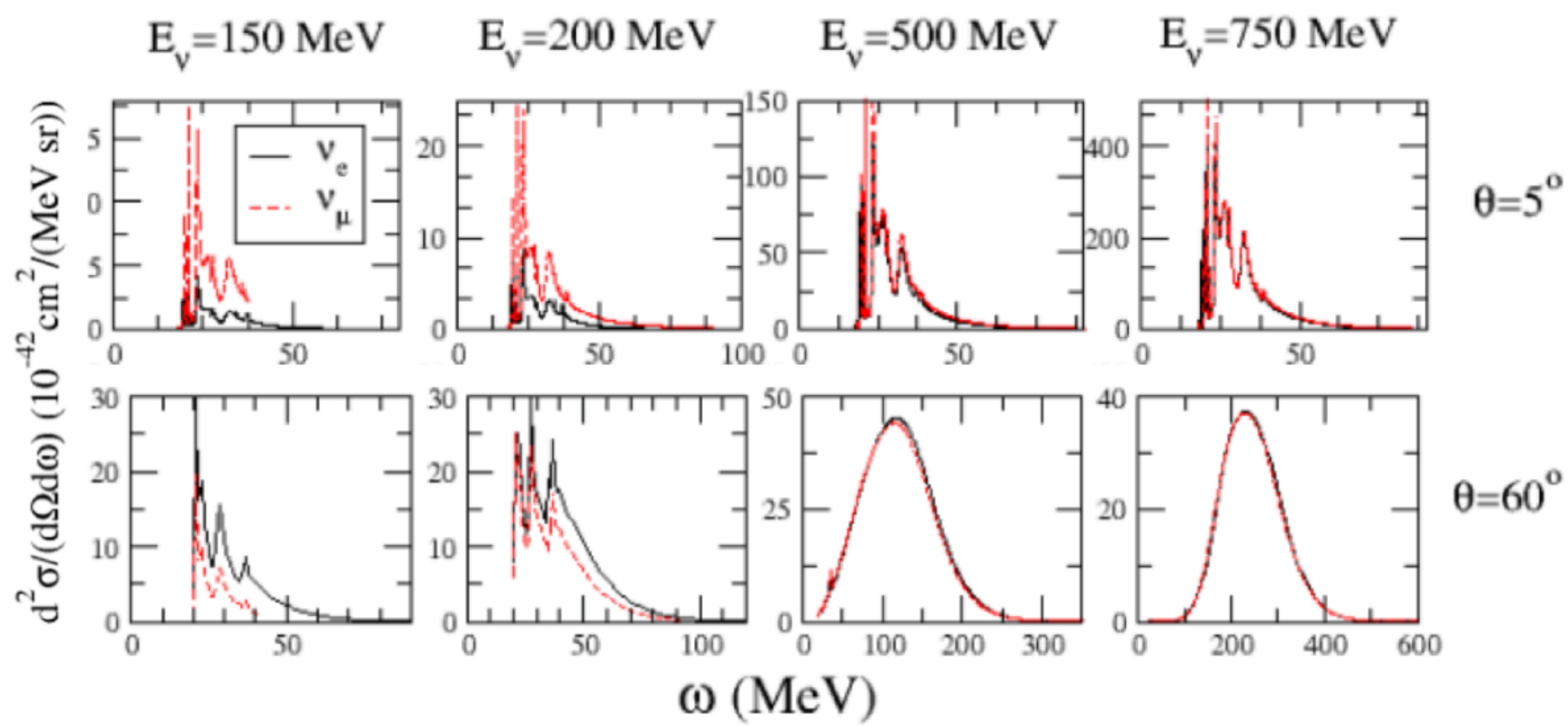

M. Martini, N. Jachowicz, M. Ericson, VP, T. Van Cuyck, N. Van Dessel, Phys. Rev. C94, 015501 (2016)

ν_e/ν_μ cross sections at low energies

- At lower energies:
  - For small scattering angles, ν_μ cross sections are higher than the ν_e ones.
  - For larger scattering angles, this behavior is opposite.

- At higher energies:
  - ν_e and ν_μ cross sections roughly coincide.

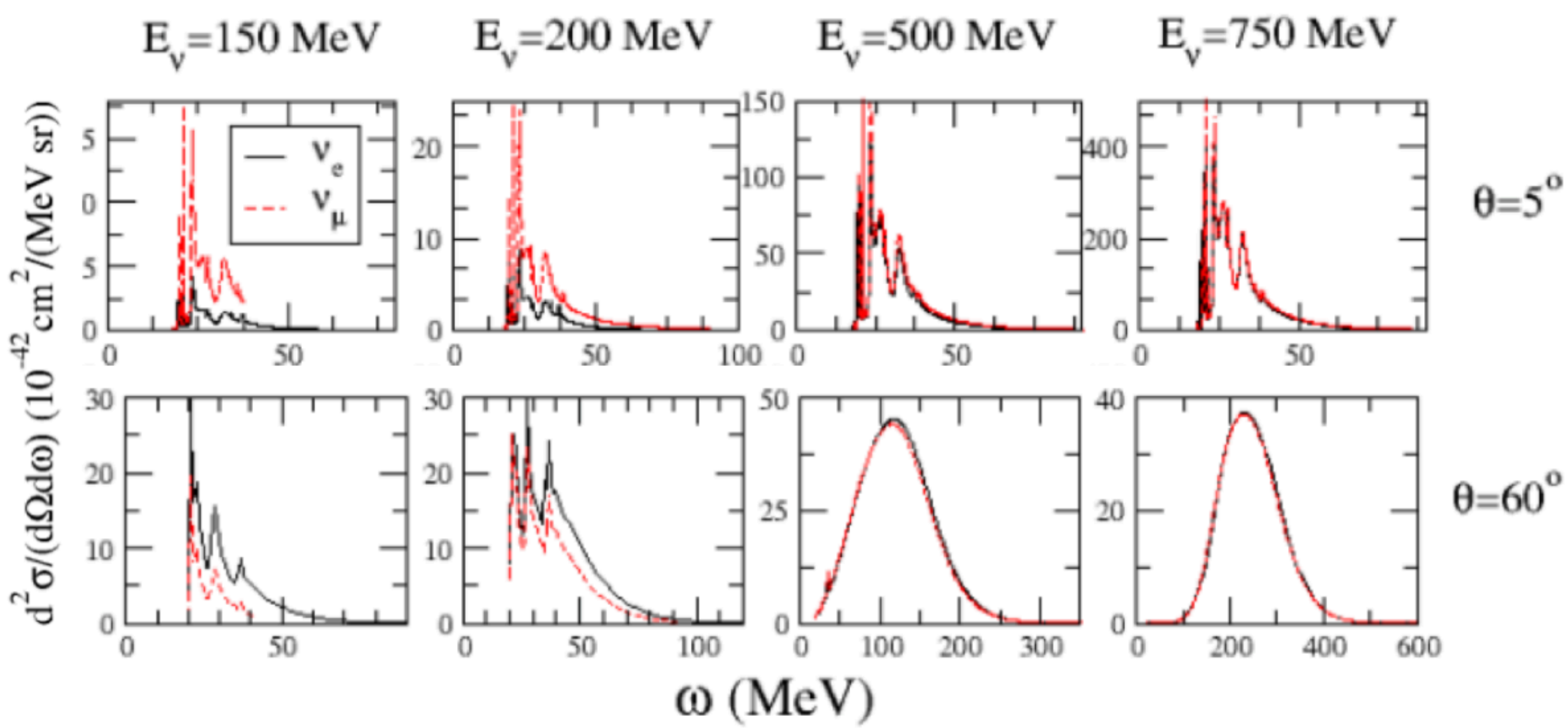

- For forward scattering, the muon mass in the final state leads to a larger momentum transfer (q), which shifts the response to larger values.

- Remember nuclear response, $R(q,\omega)$, are function of q.

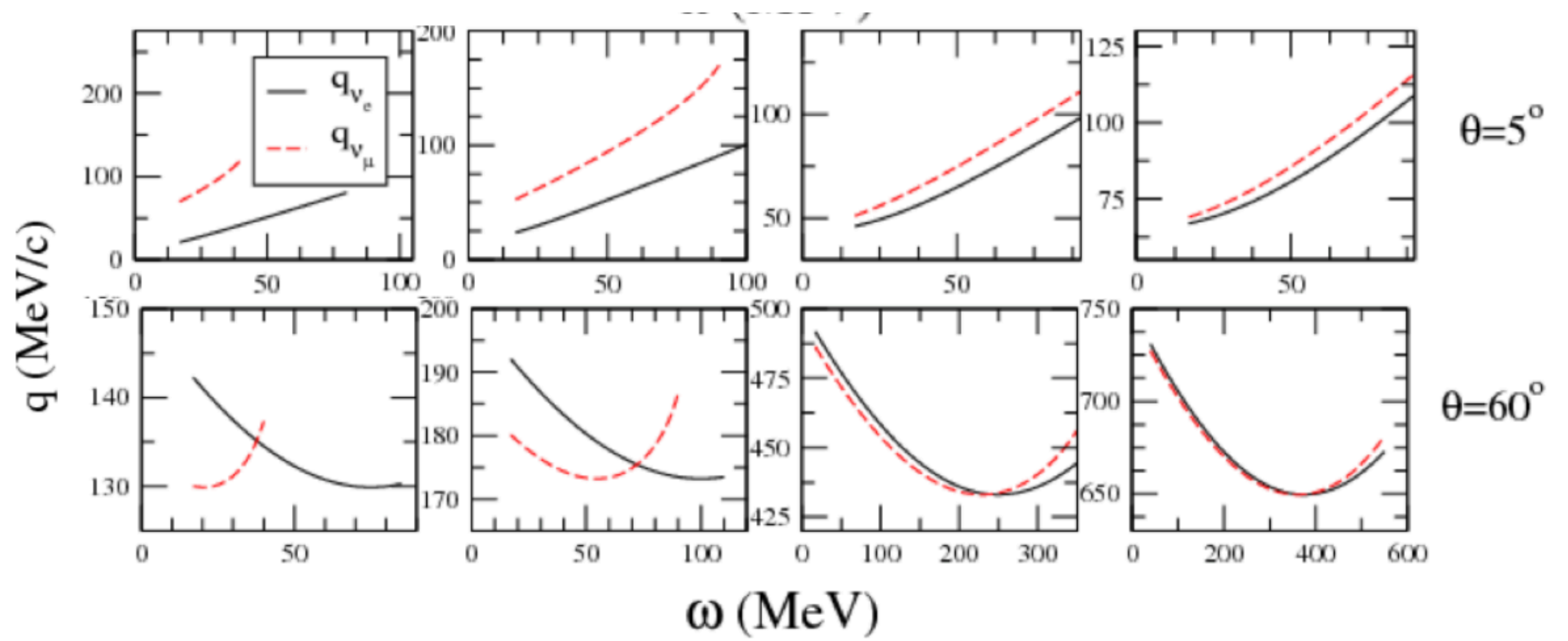

M. Martini, N. Jachowicz, M. Ericson, VP, T. Van Cuyck, N. Van Dessel, Phys. Rev. C94, 015501 (2016)

ν_e/ν_μ cross sections at low energies

- At lower energies:
  - For small scattering angles, ν_μ cross sections are higher than the ν_e ones.
  - For larger scattering angles, this behavior is opposite.

- At higher energies:
  - ν_e and ν_μ cross sections roughly coincide.

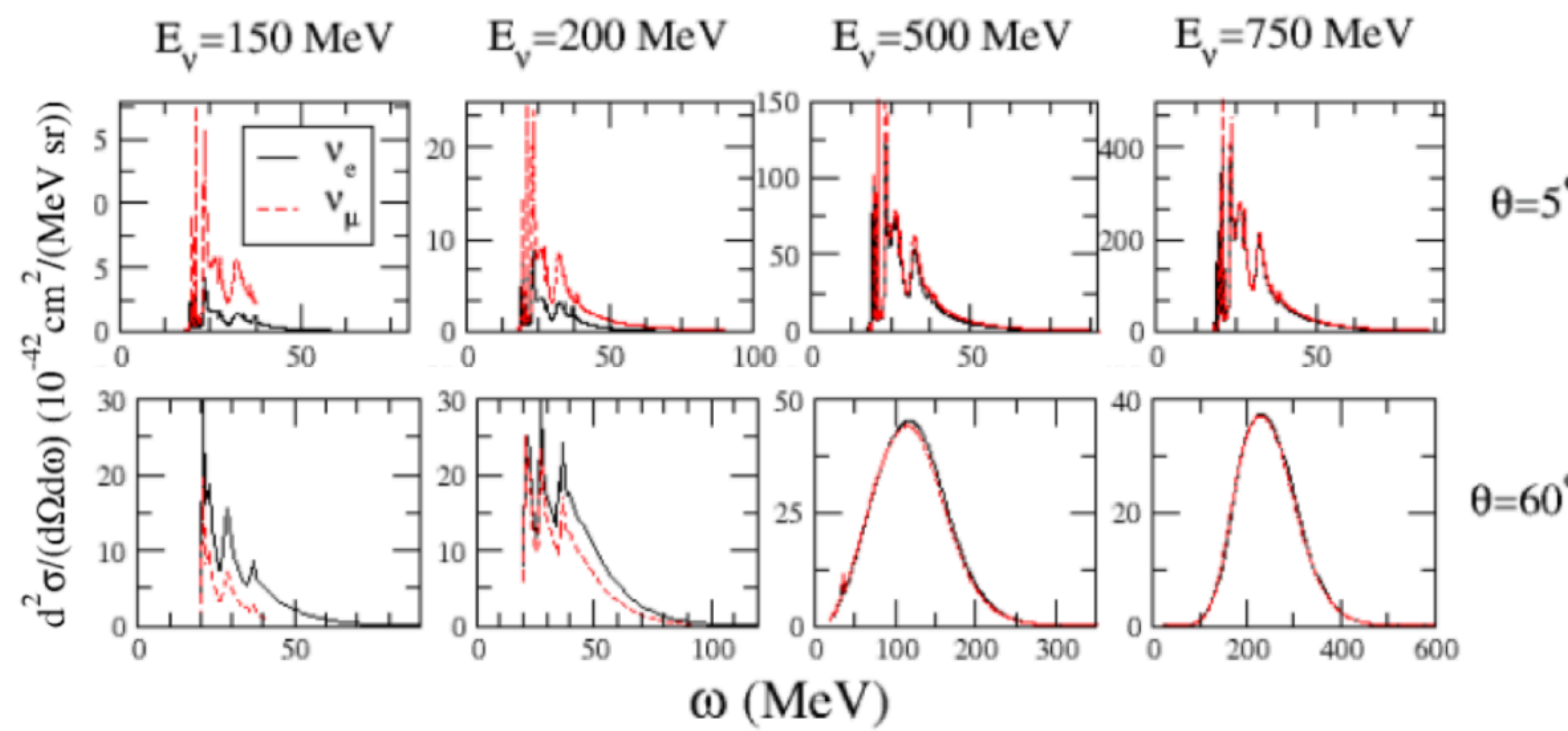

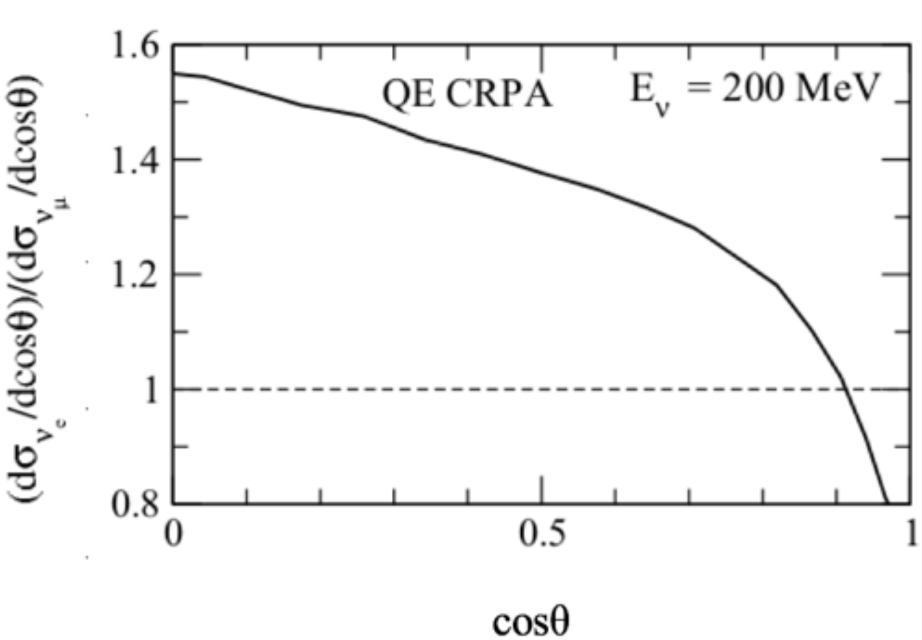

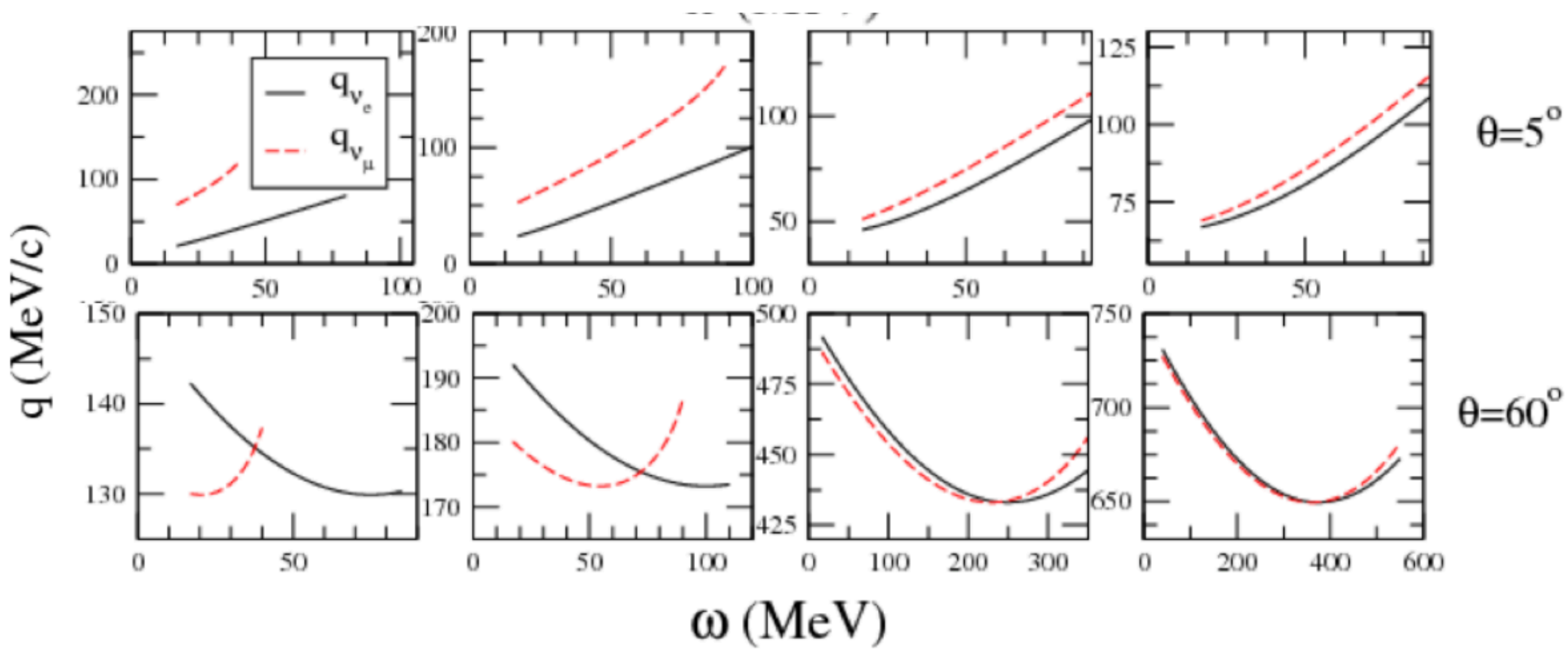

M. Martini, N. Jachowicz, M. Ericson, VP, T. Van Cuyck, N. Van Dessel, Phys. Rev. C94, 015501 (2016)

ν_e/ν_μ cross sections at low energies

- Using two independent Mean-Field approaches: RMF and HF-CRPA
  - MF approaches (in a nutshell): All bound and scattering states are obtained by solving the Schrödinger (or Dirac) equation in a central mean field potential. This means all states are consistent and orthogonal. Naturally includes: Binding, Fermi motion, Elastic final state interactions, Pauli blocking, orthogonality (both bound and scattered nucleon wave-functions are computed in the same nuclear potential).

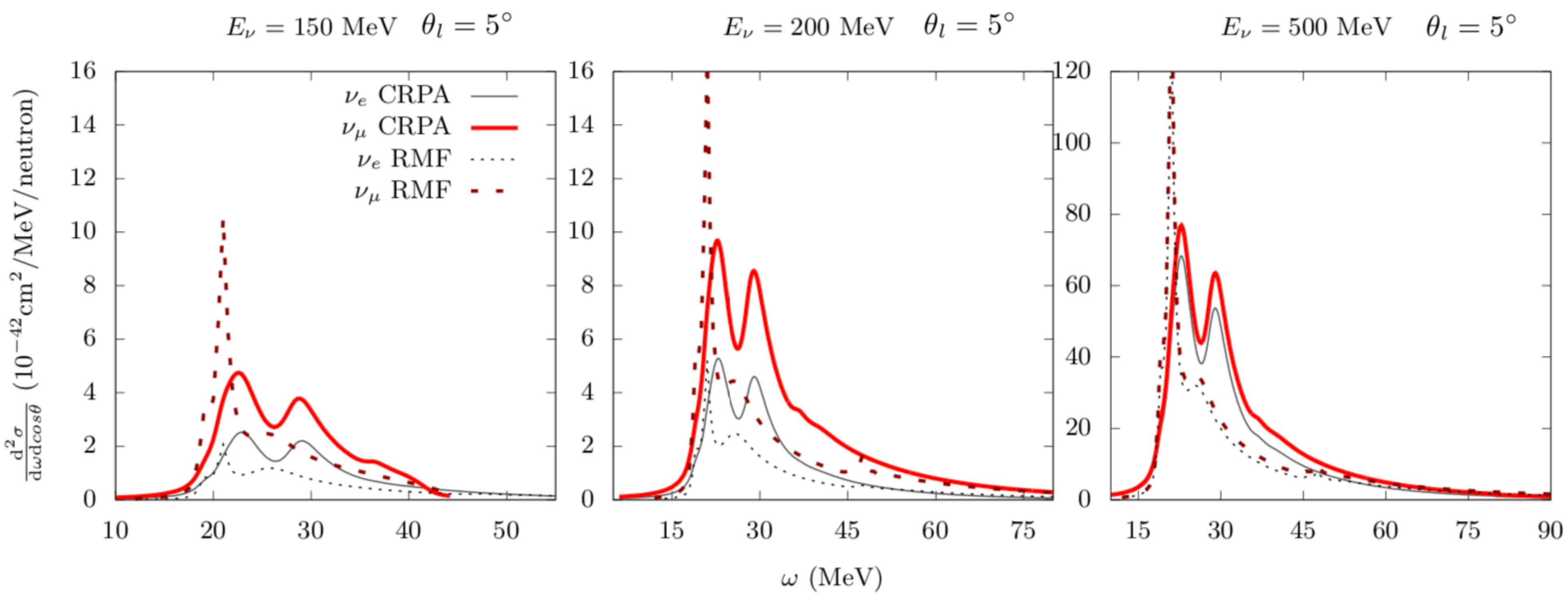

A. Nikolakopoulos, N. Jachowicz, N. Van Dessel, K. Niewczas, R. González-Jiménez, J. M. Udías, VP, Phys. Rev. Lett. 123, 052501 (2019).

- Larger ν_μ than ν_e cross sections for low ω and q (if the initial and final state wave functions are treated consistently).
  - The muon mass in the final state leads to a larger momentum transfer (q) which shifts the response to larger values.
  - Remember nuclear response, $R(q, \omega)$, are function of q.

ν_e/ν_μ cross sections at low energies

- Using two independent Mean-Field approaches: RMF and HF-CRPA
  - MF approaches (in a nutshell): All bound and scattering states are obtained by solving the Schrödinger (or Dirac) equation in a central mean field potential. This means all states are consistent and orthogonal. Naturally includes: Binding, Fermi motion, Elastic final state interactions, Pauli blocking, orthogonality (both bound and scattered nucleon wave-functions are computed in the same nuclear potential).

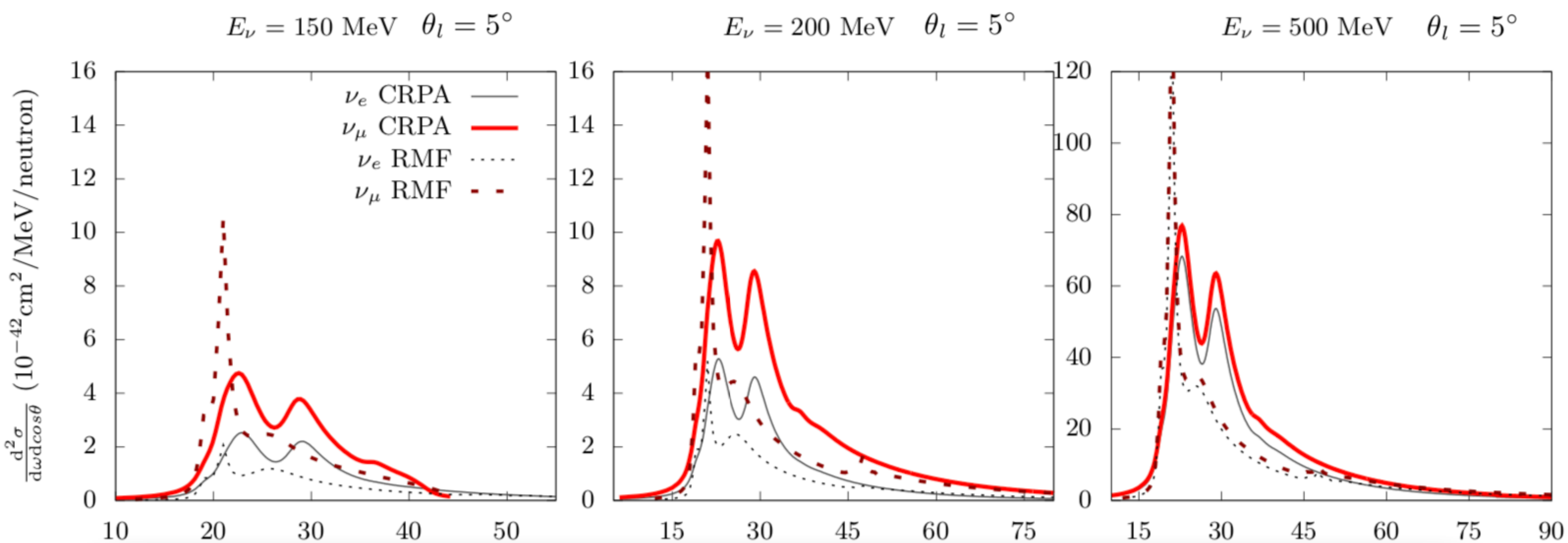

A. I ... ez,
J. I

Reminder: This is how GENIE sees this region

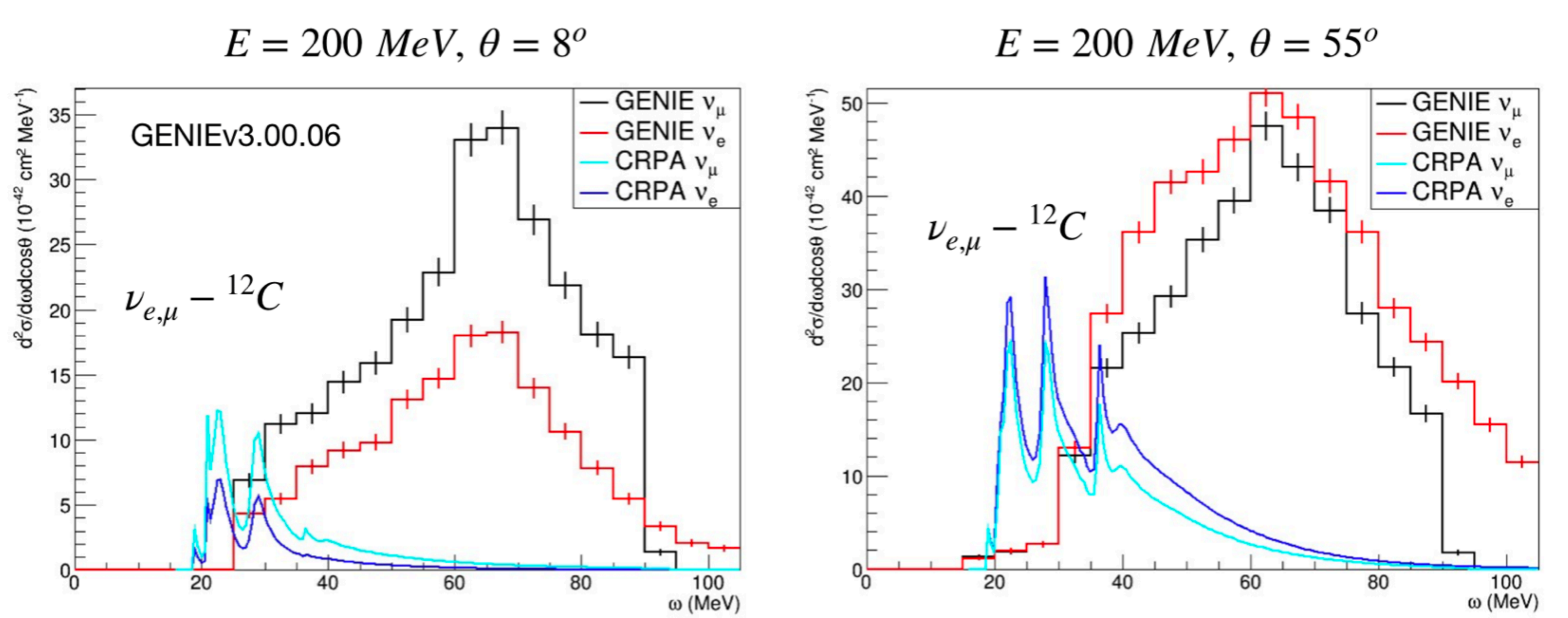

- Larger ν_μ than ν_e cr ... reated consistently).
  - The muon mass i ... ponse to larger values.
  - Remember nucle ...

Summary

- We use a microscopic nuclear many-body theory model, HF-CRPA approach, for lepton-nucleus scattering covering processes from threshold to quasielastic region for various nuclei (including ^{40}Ar).

- The model successfully describes (e,e') data for broad range of kinematics, and describes (anti)neutrino data reasonably well.

- Microscopic neutrino-nucleus models, which treat initial and final state wave functions consistently, predict larger ν_μ than ν_e cross sections for low ω and q values - its impact on observed low-energy excess is currently under investigation.

- We are working with Steven Gardiner to implementing HF-CRPA model in GENIE. Steven will share more information in his talk.

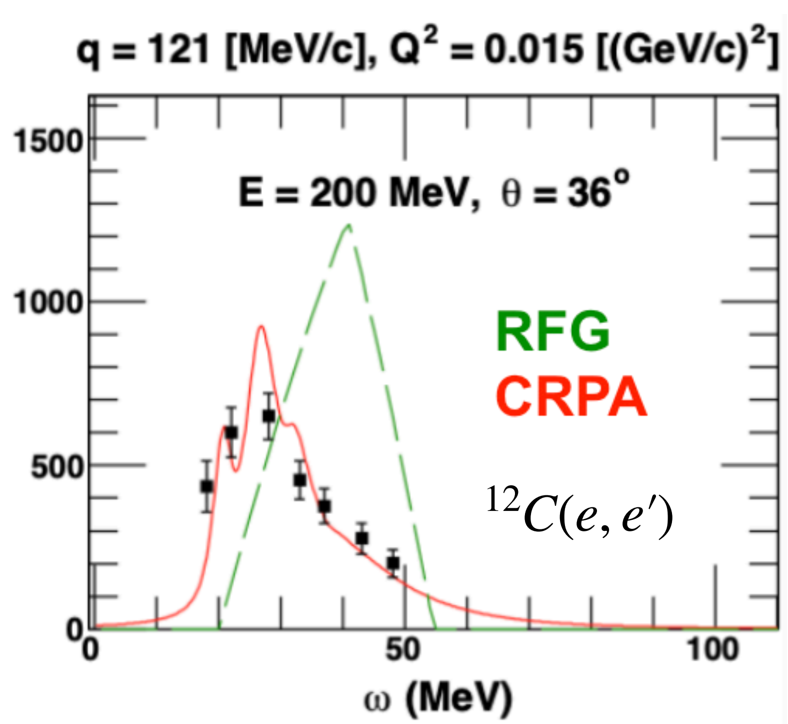

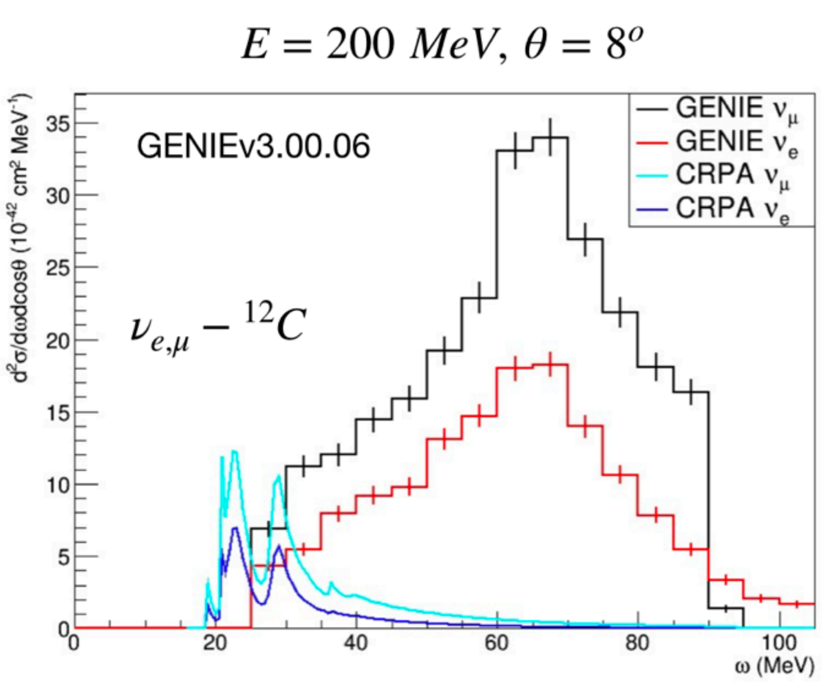

Backup Slides

HF-CRPA model in a nutshell

- Nucleons are bound in the nucleus. All bound and scattering states are obtained by solving the Schrödinger equation in a central mean field potential. Includes long-range correlation between nucleons in a self-consistent way.
- Captures the main nuclear effects in a consistent quantum mechanical way.
- Naturally includes: Binding, Fermi motion, Elastic Final State Interaction (distortion of the outgoing nucleon in real potential), Pauli blocking, and orthogonality (the nucleon wave function does not overlap with a bound state).

Fermi-gas models in a nutshell

- Relativistic global Fermi-gas: The nuclear ground state is a Fermi gas of non-interacting nucleons characterized by a fixed Fermi momentum.
- Relativistic local Fermi-gas: The nuclear ground state is a Fermi gas of non-interacting nucleons characterized by a Fermi momentum fixed according to the local density of protons and neutrons. $k_F(r) \approx \left(3/2\pi^2 \rho(r)\right)^{1/3}$
- Constant binding energy.

Low-energy lepton-nucleus scattering

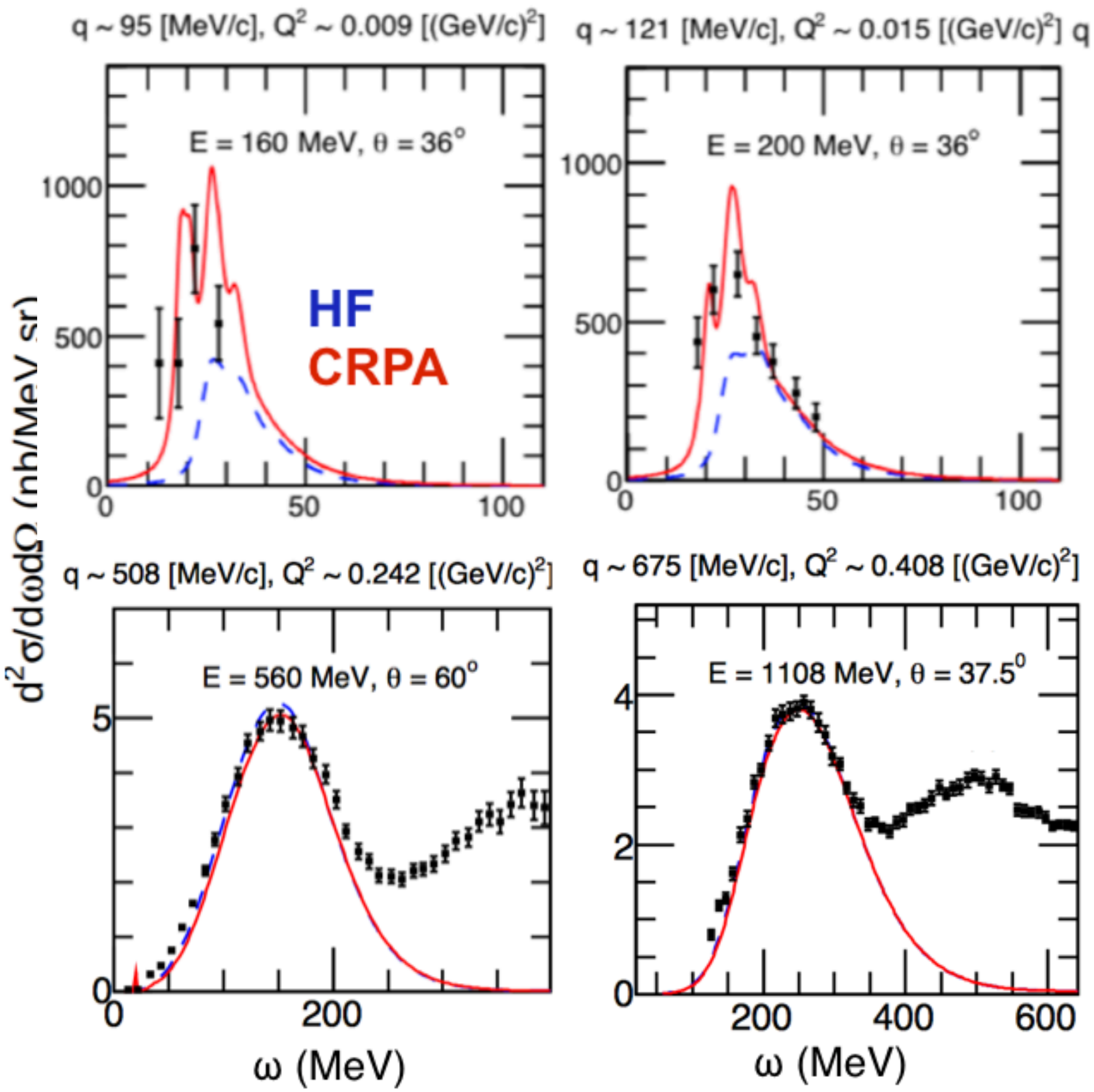

- **Comparing Relativistic global Fermi Gas vs CRPA**

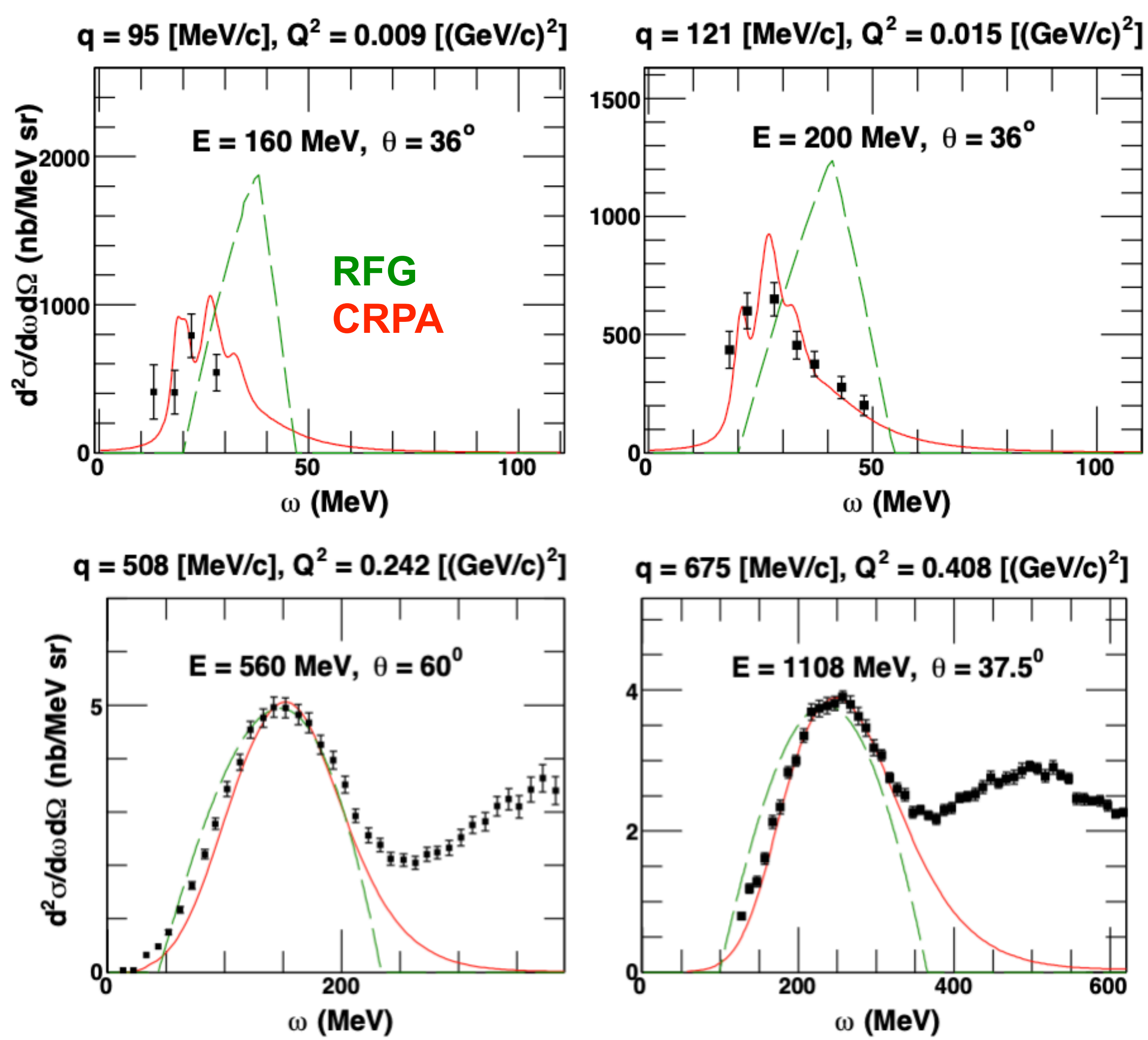

VP, N. Jachowicz, T. Van Cuyck, J. Ryckebusch,
M. Martini, Phys. Rev. C92, 024606 (2015)

Low-energy lepton-nucleus scattering

- $^{12}C\ (\nu_\mu, \mu^-)$ cross section
- **Comparing Relativistic *local* Fermi Gas vs CRPA**

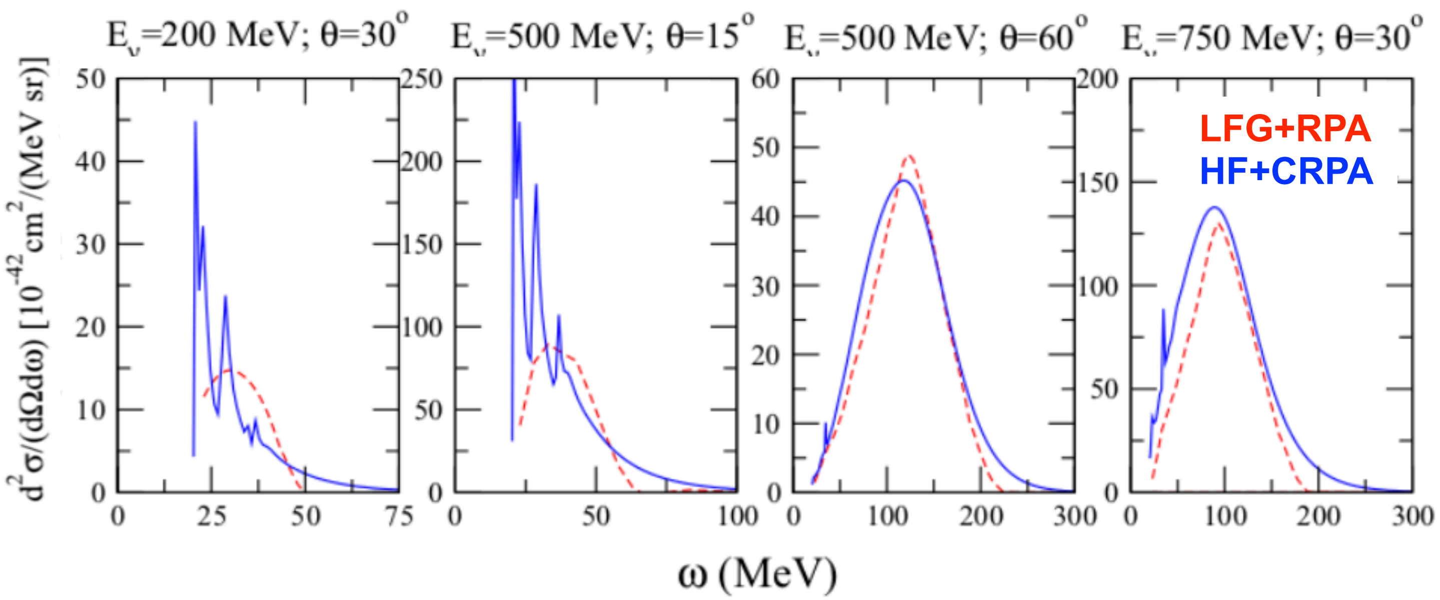

M. Martini, N. Jachowicz, M. Ericson, VP, T. Van Cuyck, N. Van Dessel, Phys. Rev. C94, 015501 (2016)

- $^{12}C\ (e,e')$ cross section
- **Comparing Relativistic *global* Fermi Gas vs CRPA**

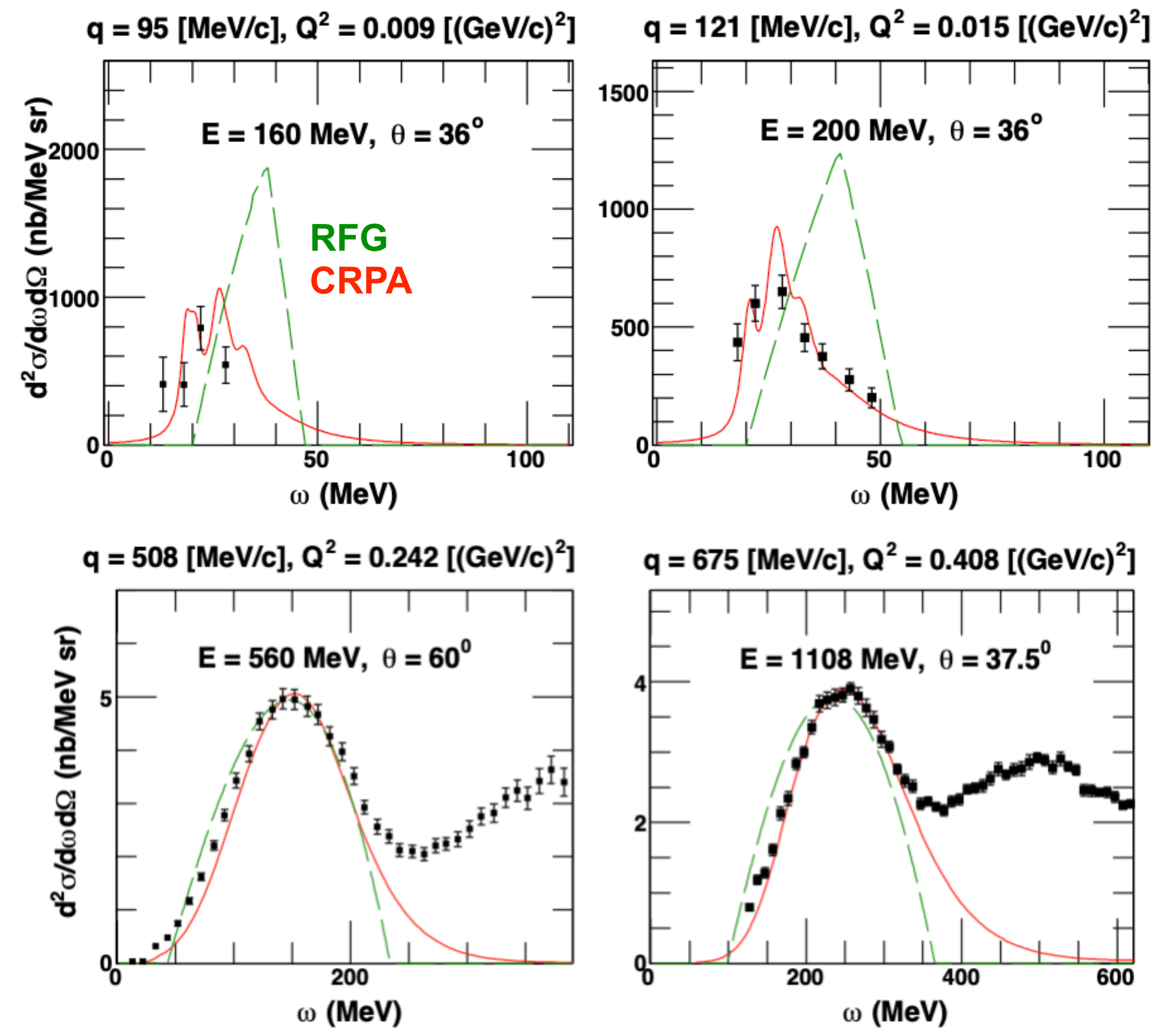

Comparing RPA-based models

RPA polarization propagator: $\Pi = \Pi^0 + \Pi^0\, V\, \Pi$

[Martini *et al.* and Nieves *et al.*]

Bare Propagator: RIFG

π exchange, ρ exchange, contact Landau-Migdal parameters

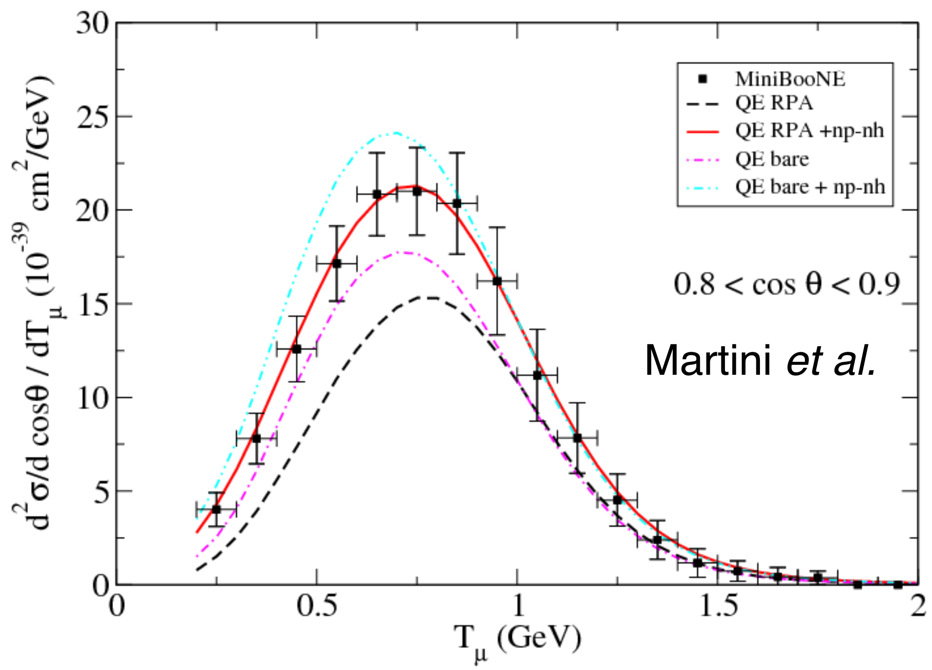

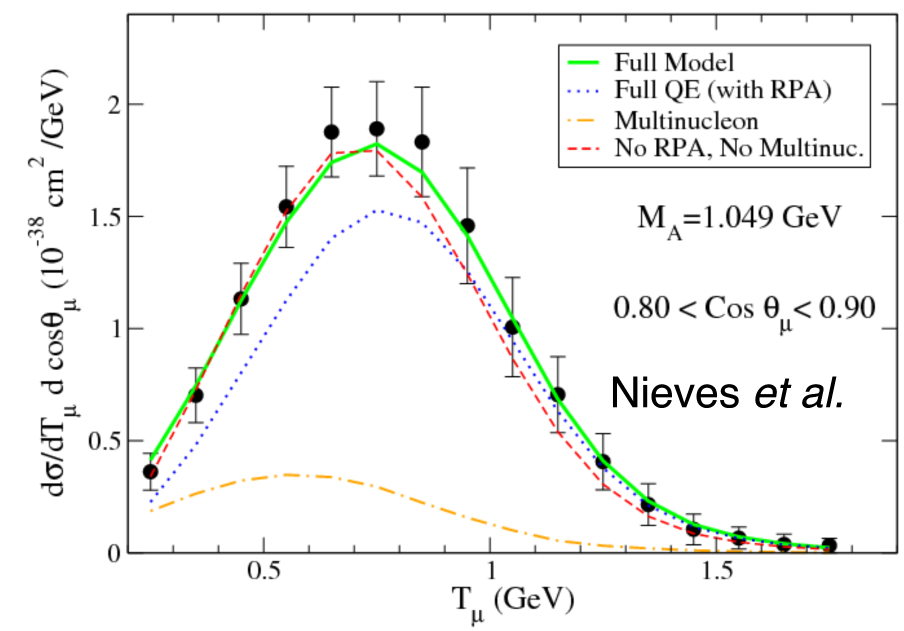

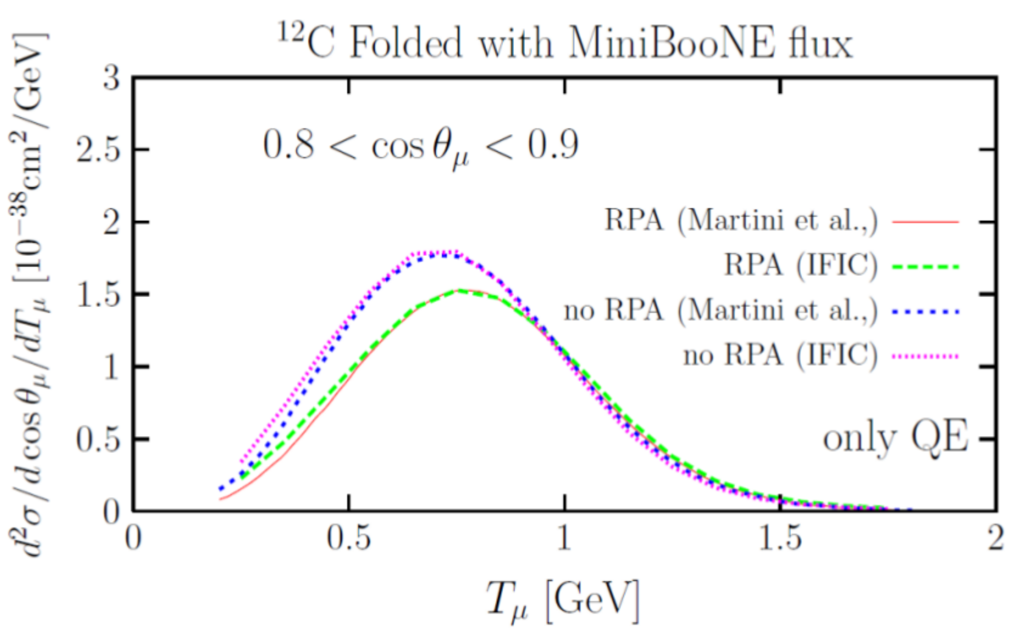

- Significant RPA quenching in both approaches.
- Genuine QE bare (RIFG) and RPA very similar in both approaches.

Comparing RPA-based models

RPA polarization propagator: $\Pi = \Pi^0 + \Pi^0 \, V \, \Pi$

[Ghent Approach]

Bare Propagator: HF

Skyrme (SkE2)

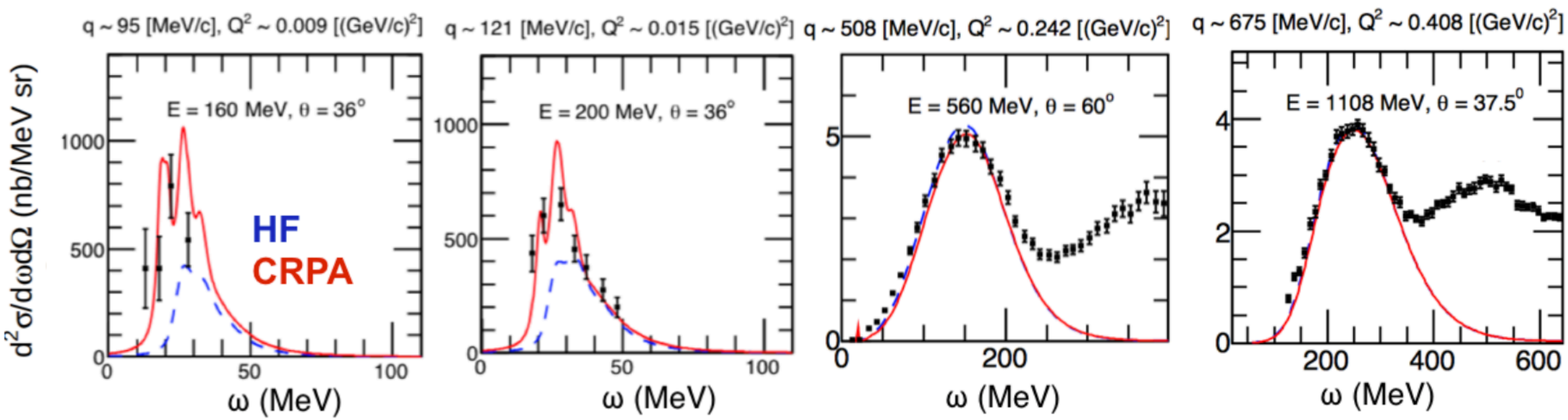

VP, N. Jachowicz, T. Van Cuyck, J. Ryckebusch, M. Martini, Phys. Rev. C92, 024606 (2015)

- At low ω, RPA (long-range correlations) describes the collective behavior of the nucleus (low-energy excitations).
- At high ω, RPA effects are smaller.
- Approach compares well with the (e,e') data.

Comparing RPA-based models

LRFG, RPA: Martini, et al.

- Important differences at both ends of the spectrum

  → Low-energy excitations at low ω

  → High ω tail

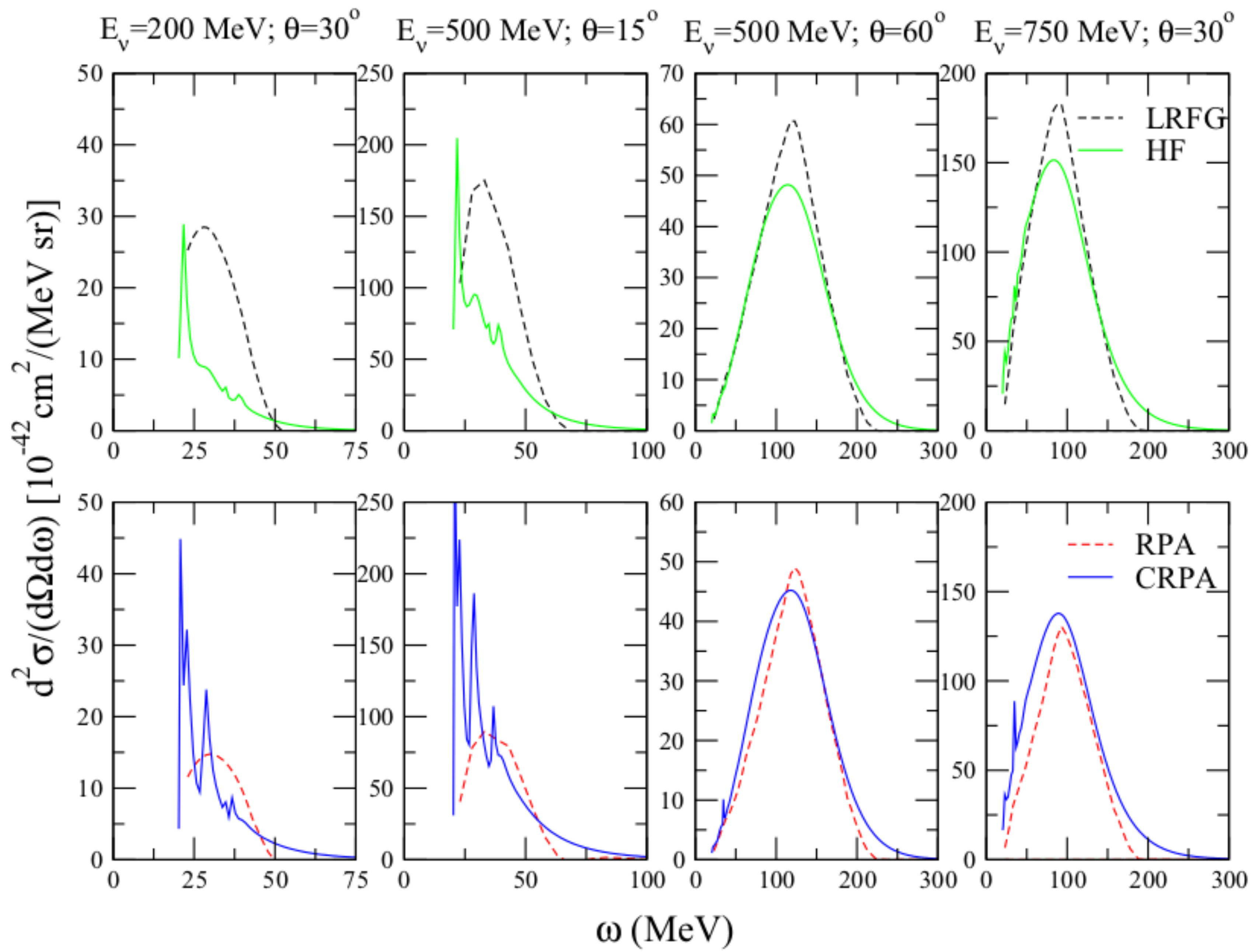

M. Martini, N. Jachowicz, M. Ericson, VP, T. Van Cuyck, N. Van Dessel, Phys. Rev. C94, 015501 (2016)

Comparing RPA-based models

Model	Starting point	N-N interaction	Shell effects	Low-energy excitations & Giant resonances	RPA effect
Martini, Ericson *et al.*	Local Fermi Gas	Meson -exhange (π,ρ,g')	No	No	Significant suppression (LLEE effect*)
Nieves *et al.*	Local Fermi Gas	Meson -exhange (π,ρ,g')	No	No	Significant suppression (LLEE effect*)
Pandey, Jachowicz *et al.*	Hartree-Fock	Skyrme	Yes	Yes	Describes low ω physics, not much effects at higher ω

- Significant differences between RPA and CRPA approach, at both ends of the (one-body) ω spectrum.

*Lorentz-Lorentz-Ericson-Ericson effect: accounts for the possibility of a Δ-hole excitation in the RPA chain

Comparing RPA-based models

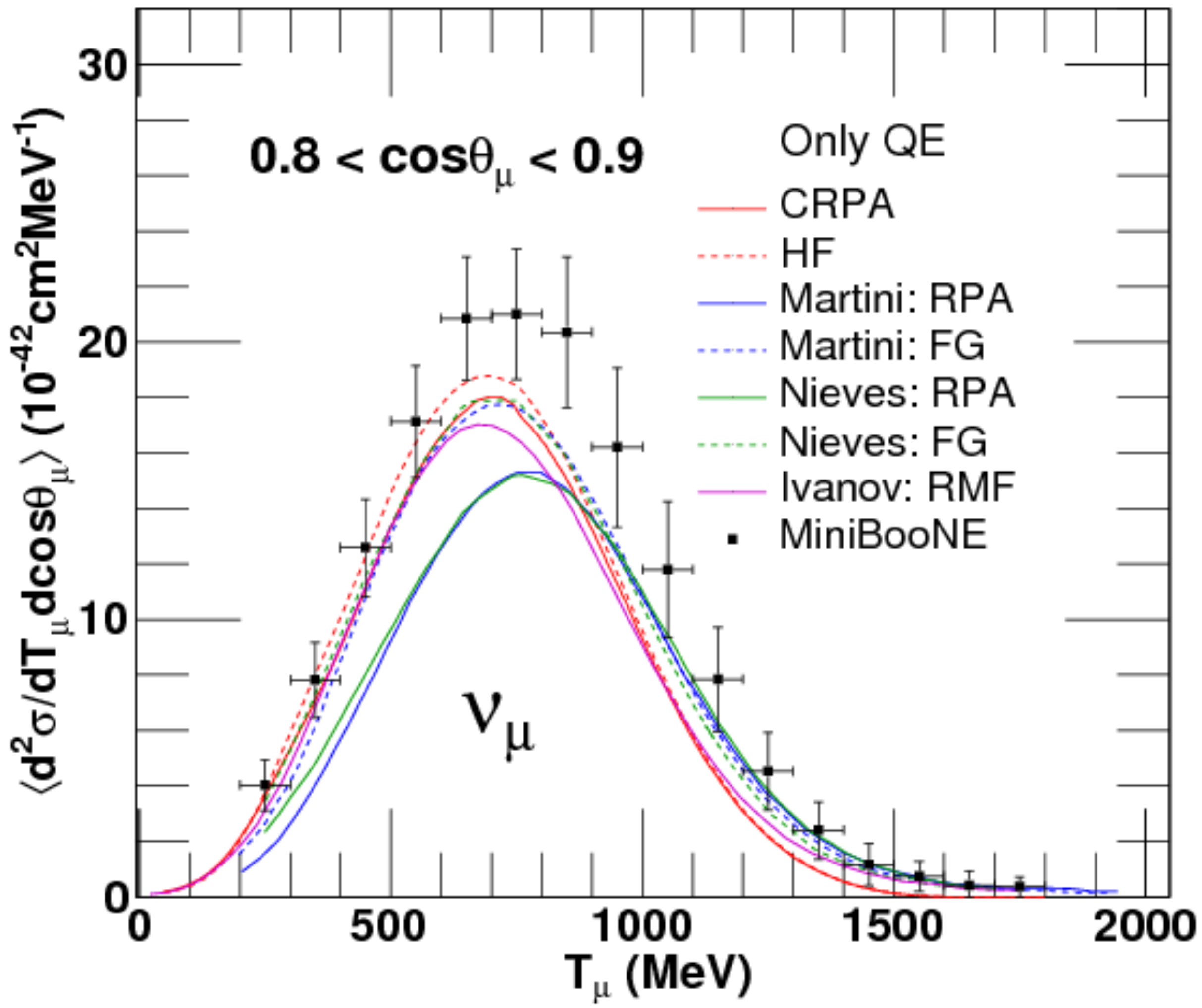

VP, N. Jachowicz, M. Martini, R. González Jiménez, J. Ryckebusch, T. Van Cuyck, and N. Van Dessel, Phys. Rev. C94, 054609 (2016)

- The pure QE RPA results of Martini *et al.* and Nieves *et al.* are significantly different from HF, CRPA and RMF (Ivanov *et al.*) results.
- These difference can be assigned to the use of a detailed microscopic nuclear model in the HF and RMF calculations compared to the FG ones.